CHAPTER 4

RESULTS

4. Results

4.1 Isolation and Screening of metal resistant bacterial strains

A total of Forty two (42) bacterial isolates representing different bacterial colonies in the soil samples collected from the nearby dwelling areas of mining sites of East Singhbhum district of Jharkhand (India) were screened for the heavy metal resistant strains by serial dilution method (Table 1). Metal resistance was determined in agar medium supplemented with the different concentrations (0.5, 1.0 and 2.0 mM) of heavy metals (Cd, Cr & Ni). In the preliminary screening all the bacterial isolates were resistant to one or more metals but among them eight (8) isolates (highlighted in Table 1) were resistant to all heavy metals and were able to grow up to the highest concentration (2.0 mM).

Table 1: Screening of metal resistant bacterial strains isolated from soils in the nearby adjoining areas of mining sites of East Singhbhum district of Jharkhand (India)

Sl. No.	Strains	Cd (mM)			Cr (mM)			Ni (mM)		
		0.5	1	2	0.5	1	2	0.5	1	2
1	JHNI4012	+	+	-	+	+	-	+	+	-
2	JHNI014	+	+	+	+	+	+	+	+	+
3	JHNI4018	+	-	-	+	+	-	+	-	-
4	JHNI40211	+	+	+	+	+	-	+	+	+
5	JHNI40215	+	+	+	+	+	+	+	+	+
6	JHNI40319	+	+	-	+	+	+	+	+	+
7	JHNI40321	+	+	-	+	+	+	+	+	+
8	JHNI40322	+	+	-	+	-	-	+	-	-
9	JHNI4053	+	+	+	+	+	+	+	+	+
10	JHNI4054	+	+	-	+	-	+	+	-	-
11	JHNI4057	+	+	+	+	-	+	+	-	+
12	JHNI40411	+	+	-	+	-	-	+	-	-
13	JHNI40415	+	-	-	+	-	-	+	-	-
14	JHNI40416	+	-	-	+	+	-	+	+	+
15	JHNI4011	+	+	+	+	+	-	+	+	-
16	JHPB6011	+	-	-	+	+	-	+	+	+

Contd…

Sl. No.	Strains	Cd (mM)			Cr (mM)			Ni (mM)		
		0.5	**1**	**2**	**0.5**	**1**	**2**	**0.5**	**1**	**2**
17	JHPB6012	+	+	-	+	-	+	+	-	+
18	JHPB6014	+	+	-	+	+	-	+	+	-
19	JHPB6029	+	+	+	+	+	+	+	+	+
20	JHPB60211	+	+	-	+	-	-	+	+	-
21	JHPB60215	+	+	-	+	+	-	+	+	+
22	JHPB60318	+	+	+	+	-	-	+	-	-
23	JHPB60320	+	+	+	+	+	-	+	+	+
24	JHHG50210	+	-	-	+	+	-	+	-	-
25	JHHG50211	+	+	-	+	-	+	+	+	+
26	JHHG50215	+	+	+	+	+	+	+	+	+
27	JHHG50216	+	+	-	+	-	-	+	+	+
28	JHHG50429	+	+	-	+	+	-	+	+	+
29	JHHG50430	+	+	+	+	+	+	+	-	-
30	JHHG50432	+	-	-	+	-	-	+	-	-
31	JHHG501	+	+	+	+	-	-	+	+	+
32	JHHG502	+	+	-	+	+	-	+	+	+
33	JHHG503	+	+	+	+	-	+	+	+	-
34	JHHG504	+	+	-	+	-	-	+	+	+
35	JHHG506	+	-	-	+	-	-	+	-	-
36	JHHG508	+	+	+	+	+	+	+	+	+
37	JHCO2R	+	+	+	+	+	+	+	+	+
38	JHCO1	+	+	-	+	-	-	+	-	-
39	JHCO2018	+	+	+	+	+	+	+	+	+
40	JHCO038	+	-	-	+	+	-	+	-	-
41	JH0215O	+	-	-	+	-	-	+	-	-
42	JH0215W	+	-	-	+	-	-	+	-	-

4.2 Identification of metal resistant strains

Based on the preliminary screening 42 (forty two) bacterial isolates were subjected to biochemical characterization and the selected strains were identified by Biolog Microbial Identification System (BMIS) and 16S rDNA sequencing, followed by phylogenetic analysis.

4.2.1 Biochemical test

Forty two (42) bacterial isolates were characterized on the basis of morphological and biochemical characteristics with the standard description in Bergey's Manual of Determinative Bacteriology (1994). The bacterial isolates were tested for Gram (+ve)/(-ve), shapes (rods or cocci) and subjected to biochemical test such as cellulase, amylase, casein hydrolysis, triple sugar, carbohydrate fermentation, H_2S production, litmus, lipid hydrolysis, catalase etc. Based on the biochemical characteristics five strains were selected (Strains: JHNI40215, JHPB6029, JHCO2018, JHCO2R, JHHG50215) with distinct biochemical characters (Table 2) and were identified by Biolog microbial identification system.

4.2.2 Biolog microbial identification system (BMIS)

Biolog microbial identification system is a versatile system and is based on the principle of numerical taxonomy and uses easy and unequivocally determinable color reactions (tetrazolium violet to vividly purple formazon) indicating metabolic activities such as oxidation of a wide range of carbon compounds. Using this system, five heavy metal resistant bacterial strains with distinct biochemical characteristics were identified as (Figure 1)

JHNI40215 - *Bacillus cereus/thuringiensis*
JHPB6029 *Bacillus pseudomycoides*
JHCO2018 - *Pseudomonas aeruginosa*
JHCO2R - *Lactobacillus kefiri*
JHHG50215 - *Staphylococcus haemolyticus*

Table 2: Biochemical characterization of bacterial strains isolated from soils nearby adjoining areas of mining sites of East Singhbhum district of Jharkhand (India).

Where, Gluc-Glucose, Lac/Suc-Lactose/Sucrose, RYX- Alkaline slant acid butt and no production of H_2S, YYX- Acid slant acid butt and no H_2S production, + : Positive and - : negative.

SL NO.	STRAINS	GRAM STAINING	CELLULASE	AMYLASE	CASEIN HYDROLYSIS	TRIPLE SUGAR IRON AGAR	CARBOHYDRATE FERMENTION	H_2S PRODUCTION	NITRATE REDUCTION A&B	Zn.	RESULT	LIPID HYDROLYSIS	CATALASE	INDOLE	METHYL RED	CITRATE	GELATINASE
1	JHNI4012	-ve, Rod	-	-	+	R, Y, X	GLUC	_	+	_	+	+	+	_	+	_	+
2	JHNI4014	-ve, Rod	_	_	+	R, Y, X	GLUC	_	+	_	+	+	+	_	+	_	+
3	JHNI4018	-ve, Rod	_	_	+	R, Y, X	GLUC	_	+	_	+	+	+	_	+	+	+
4	JHNI40211	-ve, Rod	_	_	+	R, Y, X	-	_	+	_	+	+	+	_	+	+	+
5	JHNI40215	+ve, Rod	_	_	+	R, Y, X	GLUC	_	+	_	+	+	+	_	+	+	+
6	JHNI40319	+ve, Rod	_	_	+	R,Y, X	GLUC	_	+	_	+	+	+	_	+	_	+
7	JHNI40321	-ve, Rod	_	_	+	R, Y, X	GLUC	_	+	_	+	+	+	_	+	_	+
8	JHNI40322	-ve, Coccus	_	_	+	R, Y, X	GLUC	_	+	_	+	+	+	_	+	_	+
9	JHNI4053	-ve, Rod	+	_	+	R, Y, X	GLUC	_	+	_	+	+	+	_	+	_	+
10	JHNI4054	-ve, Rod	+	_	+	R, Y, X	GLUC	+	+	_	+	+	+	_	+	_	+
11	JHNI4057	-ve, Rod	+	_	+	R, Y, X	GLUC	_	+	_	+	+	+	_	+	_	+
12	JHNI40411	-ve, Rod	+	_	+	R, Y, X	GLUC	_	+	_	+	+	+	_	+	_	+
13	JHNI40415	-ve, Rod	_	_	+	R, Y, X	GLUC	_	+	_	+	+	+	_	+	_	+
14	JHNI40416	-ve, Rod	_	_	+	R, Y, X	GLUC	_	+	_	+	+	+	_	+	_	+
15	JHNI4011	-ve, Rod	_	_	+	R, Y, X	GLUC	_	+	_	+	+	+	_	+	_	+
16	JHPB6011	-ve, Rod	_	_	+	R, Y, X	-	_	+	_	+	+	+	_	+	+	+
17	JHPB6012	-ve, Rod	_	_	+	R, Y, X	GLUC	_	+	_	+	+	+	_	+	+	+
18	JHPB6014	+ve, Rod	_	_	+	R, Y, X	GLUC	_	+	_	+	+	+	_	+	_	+
19	JHPB6029	+ve, Rod	_	+	+	R, Y, X	GLUC	_	+	_	+	+	+	_	_	+	_
20	JHPB60211	-ve, Rod	_	_	+	R, Y, X	GLUC	_	+	-	+	+	−	_	+	+	+
21	JHPB60215	-ve, Rod	_	_	+	R, Y, X	GLUC	+	−	+	−	−	+	+	+	+	+
22	JHPB60318	+ve, Rod	+	+	+	R, Y, X	GLUC	+	+	-	+	−	+	+	+	+	+

Contd…

SL NO.	STRAINS	GRAM STAINING	CELLULASE	AMYLASE	CASEIN HYDROLYSIS	TRIPLE SUGAR IRON AGAR	CARBOHYDRATE FERMENTION	H_2S PRODUCTION	NITRATE REDUCTION A&B	Zn.	RESULT	LIPID HYDROLYSIS	CATALASE	INDOLE	METHYL RED	CITRATE	GELATINASE
23	JHPB60320	-ve, Rod	-	_	+	R, Y, X	GLUC	_	+	-	+	–	+	_	+	_	_
24	JHHG50210	-ve, Rod	_	_	+	R, Y, X	GLUC	_	+	-	+		+	+	+	_	+
25	JHHG50211	-ve, Rod	_	_	+	R, Y, X	GLUC	_	+	-	+		+	_	+	_	+
26	JHHG50215	+ve, Cocci	_	+	+	Y, Y, X	DEX/SUC	_	+	–	–	+	+	+	+	_	+
27	JHHG50216	-ve, Rod	_	_	+	R, Y, X	GLUC	_	+	-	+		+	_	+	_	+
28	JHHG50429	-ve, Rod	_	_	+	R, Y, X	GLUC	_	+	-	+		+	_	+	_	+
29	JHHG50430	-ve, Rod	_	_	+	R, Y, X	GLUC	_	+	-	+		+	_	+	_	+
30	JHHG50432	-ve, Rod	_	_	+	R, Y, X	GLUC	_	+	-	+		+	_	+	_	+
31	JHHG501	-ve, Rod	_	_	+	Y, Y, X	LAC/SUC	_	–	+	–	–	+	_	+	_	_
32	JHHG502	-ve, Rod	_	_	+	Y, Y, X	LAC/SUC	_	–	+	–	–	+	_	_	_	_
33	JHHG503	-ve, Rod	_	_	+	Y, Y, X	LAC/SUC	_	–	+	–	–	+	_	_	+	_
34	JHHG504	-ve, Rod	_	_	+	Y, Y, X	LAC/SUC	_	–	+	–	–	+	_	+	+	_
35	JHHG506	-ve, Rod	_	_	+	Y, Y, X	LAC/SUC	_	–	+	–	–	+	_	_	+	_
36	JHHG508	-ve, Rod	_	_	+	Y, Y, X	LAC/SUC	_	–	+	–	–	+	_	+	_	_
37	JHCO2R	+ve, Rod	-	_	-	R, Y, X	LAC/SUC	_	+	-	+	–	+	+	_	+	_
38	JHCO1	-ve, Rod	+	_	+	R, Y, X	LAC/SUC	_	+	-	+	–	+	_	+	+	+
39	JHCO2018	-ve, Rod	_	_	+	R, R, X	LAC/SUC	_	–	-	–	–	+	_	+	+	+
40	JHCO038	-ve, Rod	+	_	+	R, Y, X	LAC/SUC	_	+	-	–	–	+	_	_	+	+
41	JH0215O	-ve, Rod	_	_	-	Y, Y, X	LAC/SUC	_	–	+	–	–	+	_	_	_	_
42	JH0215W	+ve, Rod	_	_	-	R, R, X	LAC/SUC	_	–	+	–	–	+		_	_	_

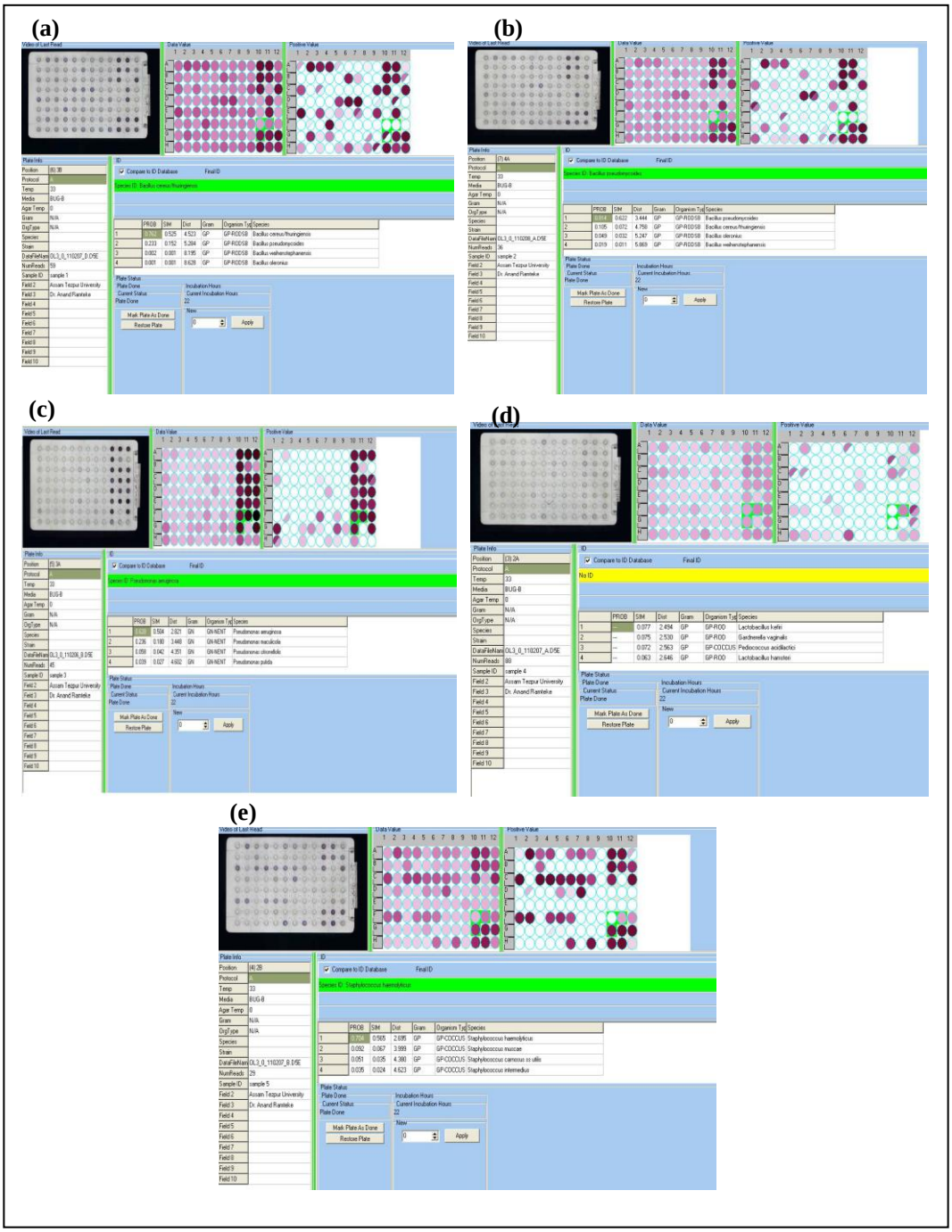

Figure 1: Metal resistant bacterial strains were identified as (a) *Bacillus cereus/thuringiensis*, (b) *Bacillus pseudomycoides*, (c) *Pseudomonas aeruginosa*, (d) *Lactobacillus kefiri*, (e) *Staphylococcus haemolyticus*; using Biolog microbial identification system.

4.2.3 16S rDNA sequencing and Phylogenetic analysis

Based on the biolog identification and their ability to grow at highest concentration of metals (Cd, Cr & Ni) *Pseudomonas* sp. (JHCO2018) and *Bacillus* sp.(JHNI40215) were selected and their 16S rDNA were amplified by PCR using universal primers and the ~1.5kb rDNA fragment were sequenced (Figure 2) and subjected to phylogenetic analysis. 16S rDNA sequence data of the two bacterial strains (JHCO2018 & JHNI40215) were analyzed and compared with the existing data base of GenBank, NCBI. Bootstrap consensus sequence was drawn by multiple sequence alignment with neighbor-joining method using software CLC sequence viewer with different bacterial species. The JHCO2018 was identified as *Pseudomonas aeruginosa* RV3 (accession no. JX313019) and JHNI40215 as *Bacillus cereus* NI40215 (accession no. KT072743) having 99% identity of the 16S rDNA sequences with the corresponding sequences of *Pseudomonas* sp. and *Bacillus* sp. (Figure 3 & 4).

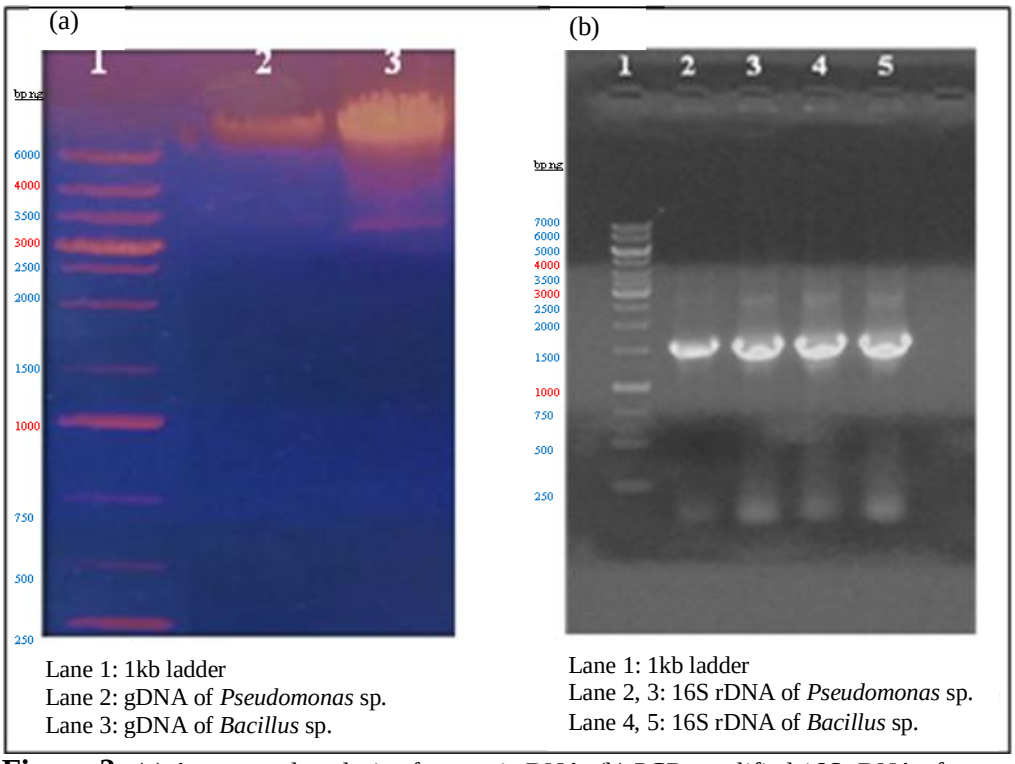

Figure 2: (a) Agarose gel analysis of genomic DNA, (b) PCR amplified 16S rDNA of *Pseudomonas* sp. (JHCO2018) & *Bacillus* sp. (JHNI40215)

TAACGGCCAAGTCCGAGGCGGATGAAGGGAGCTTGCTCCTGGATTCAGCGGCGGACGGGTGAGTAA
TAAAAAAGGAATCTGCCTGGTAGTGGGGGATAACGTCCGGAAACGGGAGCTAATACCGCATACGTC
CTGAGGGAGAAAGTGGGGGATCTTCGGACCTCACGCTATCAGATGAGTCTCTTGATAAAAAAAACTA
GTTGGTGGGGTAAAGGCCTACCAAGGCGACGATCCGTAACTGGTCTGAGAGGATGATCAGTCACACT
GGAACTGAGACACGGTCCAGACTCCTACGGGAGGCAGCAGTGGGGAATATTGGACAATGGGCGAAA
GCCTGATCCTTTTATGCCGCGTGTGTGAAGAAGGTCTTCGGATTGTAAAGCACTTTATTTTGGGAGGA
AGGGCAGTAAGTTAATACCTTGTTTGTTTTTGACGTTACCAACAGAATACCCACCGGTTATTTTCGTG
CCAACAGCCCCCCCCCCCTACGAAGGGTGCAAGCGTTAATCGGAATTACTGGGCGTAAAGCGCGCGT
AGGTGGTTCACAAGTTGGATGTGAAATCCCCGGGCTCAACCAGTAGAACTGCATCCAAAACTACTGA
GCTAGAGTACGGTACATTGTTGGTGGAATTTCCTGTGTAGCGGTGAAATGCGTAGATATAGGAAGGA
ACACCAGTGGCGAAGGCGACCACCTGGACTGATACTGACACTGAGGTGCGAAAGCGTGGGGAGCAA
ACAGGATTAGATACCCTGGTAGTCCACGCCGTAAACGATGTCGACTAGCCGTTGGGATCCTTGAGAT
CTTAGTGGCGCAGCTAACGCGATAAGTCGACCGCCTGGGGAGTACGGCCGCAAGGTTAAAACTCAA
ATGAATTGACGGGGGCCCGCACAAGCGGTGGAGCATGTGGTTTAATTCGAAGCAACGCGAAGAACC
TTACCTGGCCTTGACATGCTGAGAACTTTCCAGAGATGGATTGGTGCCTTCGGGAACTCAGACACAG
GTGCTGCATGGCTGTCGTCAGCTCGTGTCGTGAGATGTTGGGTTAAGTCCCGTAACGAGCGCAACCC
TTGTCCTTAGTTACCAGCACCTCGGGTGGGCACTCTAAGGAGACTGCCGGTGACAAACCGGAGGAAG
GTGGGATGACGTCAAGTCATCATGGCCCTTACGGCCAGGGCTACACACGTGCTACAATGGTCGGTAC
AAAGGGTTGCCAAGCCGCGAGGTGGAGCTAATCCCATAAAAAAAATCGTAGTCCGGATCGCAGTCT
GCAACTCGACTGCGTGAAGTCGGAATCGCTAGTAATCGTGAATCAGAATGTAAACGGTGAATACGTT
CCCGGGCCTTGTACACACCGCCCTTCACACCATGGGAGTGGGTTGCTCCAGAAGTAGCTAGTCTAAC
CGCAAGGGGGACGGTTACCCACGGATGGGTTTACGGTA (1441 bp)

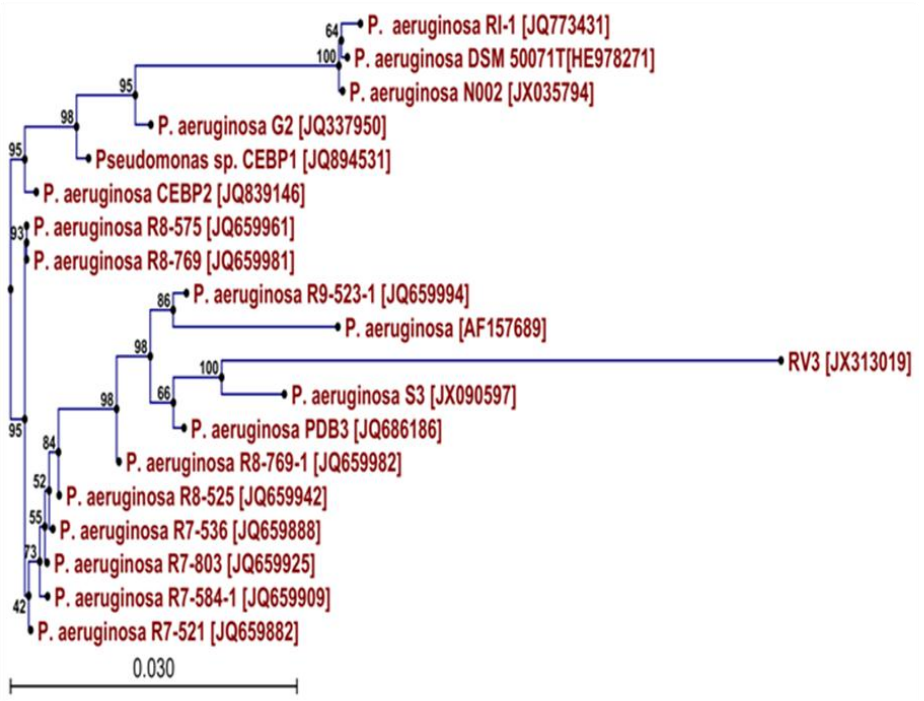

Figure 3: Neighbor joining tree based on 16S rDNA gene sequences, showing relationship of strain *Pseudomonas aeruginosa* RV3 with closely related strains of *Pseudomonas aeruginosa.* The data set was resampled 1000 times by using the boot strap option and percentage of boot strap values are given at nodes.

TGGGGCGGGGCCTAATTACATGCAAGTCGAGCGAATGGATTAAGAGCTTGCTCTTATGAAGTTAGCGGCGGACGGG
TGAGTAACACGTGGGTAACCTGCCCATAAGACTGGGATAACTCCGGGAAACCGGGGCTAATACCGGATAACATTTT
GAACCGCATGGTTCGAAATTGAAAGGCGGCTTCGGCTGTCACTTATGGATGGACCCGCGTCGCATTAGCTAGTTGGT
GAGGTAACGGCTCACCAAGGCAACGATGCGTAGCCGACCTGAGAGGGTGATCGGCCACACTGGGACTGAGACACGGC
CCAGACTCCTACGGGAGGCAGCAGTAGGGAATCTTCCGCAATGGACGAAAGTCTGACGGAGCAACGCCGCGTGAGTG
ATGAAGGCTTTCGGGTCGTAAAACTCTGTTGTTAGGGAAGAACAAGTGCTAGTTGAATAAGCTGGCACCTTGACGG
TACCTAACCAGAAAGCCACGGCTAACTACGTGCCAGCAGCCGCGGTAATACGTAGGTGGCAAGCGTTATCCGGAATT
ATTGGGCGTAAAGCGCGCGCAGGTGGTTTCTTAAGTCTGATGTGAAAGCCCACGGCTCAACCGTGGAGGGTTCATTT
GATAGCTGGGAGATCTAGCGTGCAAGAGGGAGGAAAGTGGAATTACCATGTGTAGCTGATGAATTGCGTAGAGGAA
TGACGGACTACCTGTGGCGAGGTGGTCTTCTGGTTTTGTAACTGTCAGTGAGAGTTGAAACCTGGGAAGCACCCAG
GATTAGATACCTTGTCAGTCCATGCGGTAAACGATGAGTGATACGTGTAAGAGGGTTTCCGCCTTTTAGTGTCAAG
TTTAACCCATTACCCATTCCCCCCGGGGATGAGGCCTGCAAGGTCAAATCTCAAAGGAAAACCGGGGGCCCGCCCAA
GCGGTGGAGCATTTGGTTAAATTGGAAGCAACGGGAGGACCCTTGCCGGTTCTGGCAATCTTTTAACAACCCTAGA
AAAAGGAGTTTTCGTTAGGGAGCCAAGTGACAGAAGTAGCATGTTTTTTTCAGTCAACAGATGAGATGTTGGGTTA
AGTCCGGCAAGGAGGGCAACCTTGGTTCTTCAGACCCTCCTTCAATTTGGCCATTTTAAGGTGGCTGCCGGCGCCAA
GAGGGAGGAAGGTGGGTCAGTCGTCAAATCACCGATCCCCTTATCACGTGGGTAACACCTGTGTTCCAAGGGGAGG
TACAAAGTCACCCAAGACCTAATGGGGGACTTATTTTTTTAAACCCGACACCATTTCGGATTGTAGGAAGCAATTCG
CATACAGGAAAAAGGAATATCTTAGAATTCGGGGATGTTTCATGCCGCGGTGAACAGTTTCCCGGCCGGGTCCACAC
GTCCAGTCACACCTCGGGAGTTAAACCACTAAGAGCAAGGTGGGGTACCATCGGAGCCAGCCGATTAGAGACTGTCG
CAAACTGC (1462 bp)

Figure 4: Neighbor joining tree based on 16S rDNA gene sequences, showing relationships of strain *Bacillus cereus* NI40215 with closely related strains of *Bacillus* sp. The data set was resampled 1000 times by using the boot strap option and percentage of boot strap values are given at nodes.

4.3.1 Determination of optimal growth conditions for *Pseudomonas aeruginosa* RV3 and *Bacillus cereus* NI40215

The optimal growth conditions with reference to pH and temperature were determined. The bacterial strains were grown in LB medium with varying pH values viz. 5, 6, 7, 8 & 9 and incubated at temperatures 28, 37 & 45 °C. Based on the growth data, the optimal pH and temperature of both the strains *Pseudomonas aeruginosa* RV3 and *Bacillus cereus* NI40215 were found to be at pH 7 and 37 °C (Figure 5 & 6).

4.3.2 Determination of Antibiotic sensitivity for *Pseudomonas aeruginosa* RV3 and *Bacillus cereus* NI40215

Antibiotic sensitivity of heavy metal resistant bacterial strains was determined by the disc diffusion method. Based on the zone of inhibition, it was observed that *Pseudomonas aeruginosa* RV3 shows resistance to a number of antibiotics such as ampicillin, erythromycin, oxacillin, clindamycin etc. as compared to *Bacillus cereus* NI40215, which is resistant only to three antibiotics (ampicillin, ceftazidime and sulphatriad) (Figure 7 & Table 3).

4.3.3 Effect of Metals (Cd, Cr & Ni) on the growth and determination of MIC for the *Pseudomonas aeruginosa* RV3 and *Bacillus cereus* NI40215

The MICs of metals (Cd, Cr & Ni) for the two bacterial strains were determined by the agar dilution method (Figure 8). MIC of metals Cd, Cr and Ni for *Pseudomonas aeruginosa* RV3 are 2.2, 2.4 & 2.8 mM respectively and for *Bacillus cereus* NI40215 are 2.1, 2.0 & 2.4 mM respectively. The order of toxicity of the metals to the bacterial strains were found to be Cd > Cr > Ni.

The growth response of *Pseudomonas aeruginosa* RV3 and *Bacillus cereus* NI40215 to different concentrations (0.5 and 2.0 mM) of heavy metals (Cd, Cr & Ni) were studied in the liquid culture medium.

The bacterial strains were cultured in presence of heavy metals for 48 h and growth rate was calculated (Figure 9). Both the bacteria showed significant decrease in the growth rate for Cd, Cr and Ni. The present data suggests slower growth of bacterial strains in the presence of metal particularly Cd, Cr and Ni (Table 4).

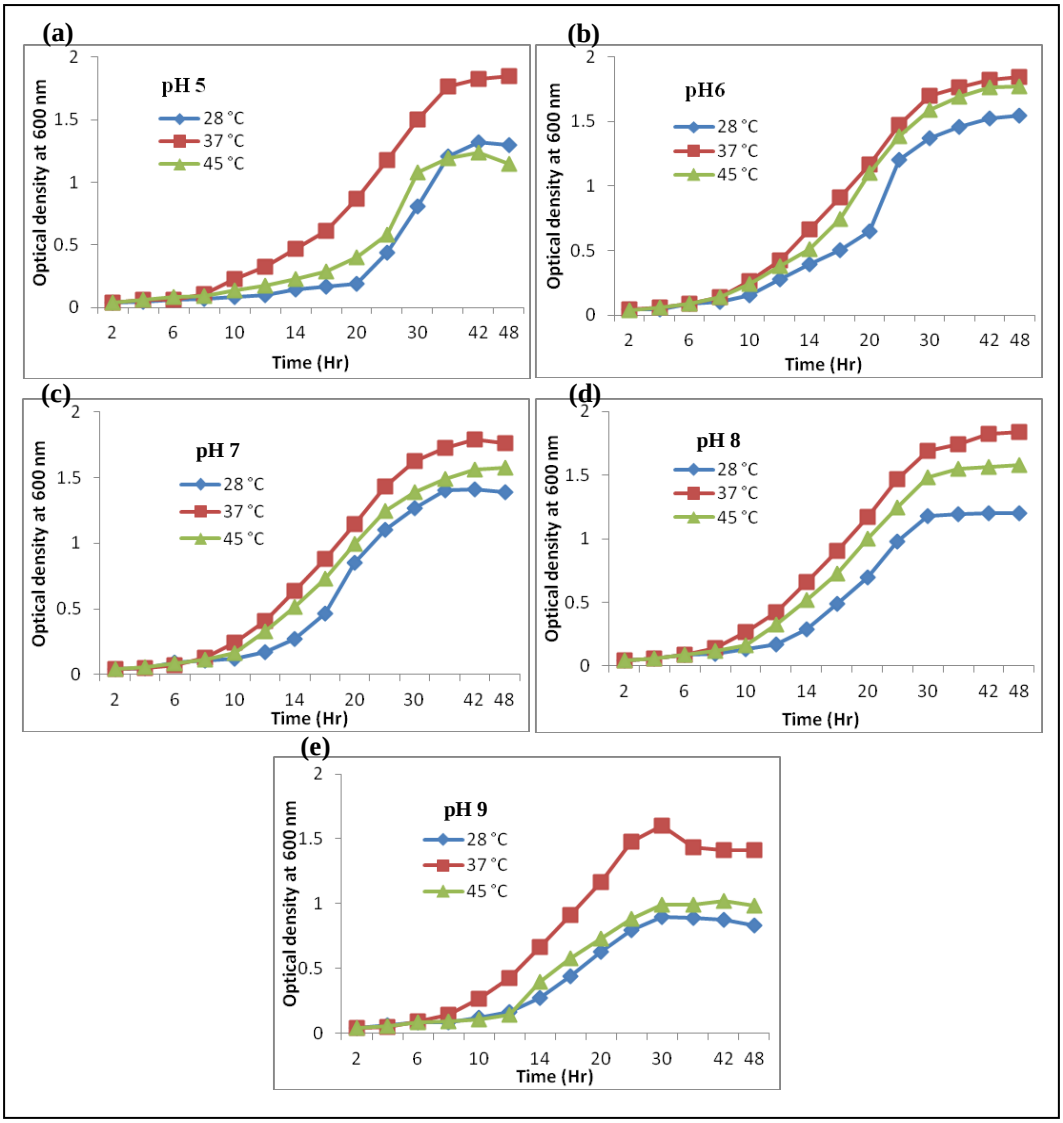

Figure 5: Effect of pH & temperature on the growth of *Pseudomonas aeruginosa* RV3.

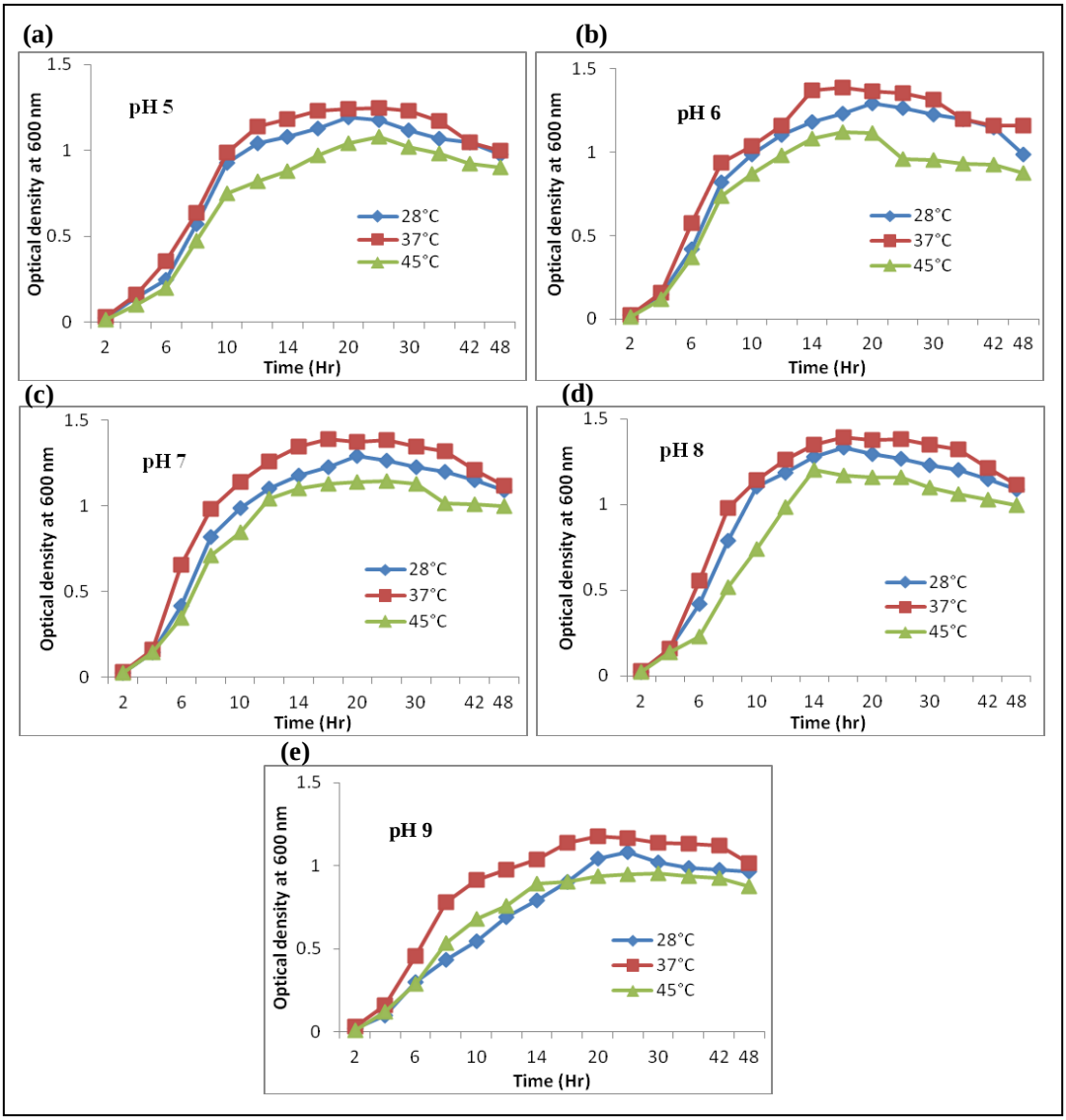

Figure 6: Effect of pH & temperature on the growth of *Bacillus cereus* NI40215.

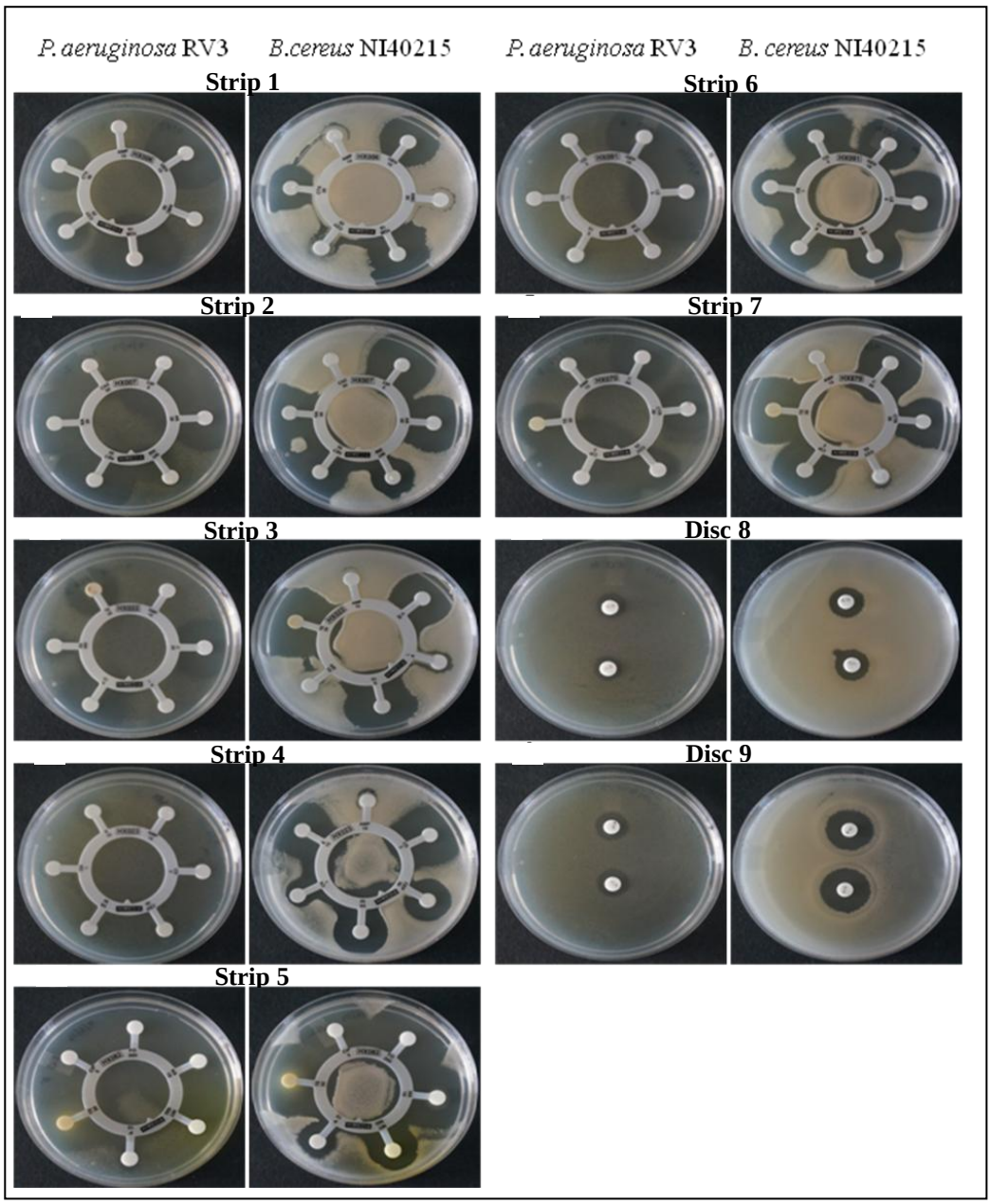

Figure 7: Antibiotic sensitivity tests of *Pseudomonas aeruginosa* RV3 & *Bacillus cereus* NI40215

Strip 1: AMP, AMC, CTX, COT, GEN, TOB
Strip 2: CAZ, CIP, AK, NIT, NET, NA
Strip 3: AMP, C, P, S, S3, TE
Strip 4: AMP, CEP, CD, E, OX, VA
Strip 5: CIP, FO, NIT, NX, P, TE
Strip 6: CD, E, GEN, LE, OX, VA
Strip 7: AMP, CTR, C, CIP, COT, TE
Disc 8: R
Disc 9: K

Table 3: Antibiotic sensitivity profile of heavy metal tolerant bacteria *Pseudomonas aeruginosa* RV3 & *Bacillus cereus* NI40215

Sl No.	Antibiotic	Abbreviation	Conc.	Zone of inhibition	
				***Pseudomonas aeruginosa* RV3**	***Bacillus cereus* NI40215**
1	Ampicilin	AMP	10 µg	Resistant	Resistant
2	Amoxyclav	AMC	30 µg	Resistant	10 mm
3	Cefotaxime	CTX	30 µg	23 mm	21 mm
4	Co-Trimoxazole	COT	25 µg	17 mm	11 mm
5	Gentamicin	GEN	10 µg	33 mm	25 mm
6	Tobramycin	TOB	10 µg	34 mm	25 mm
7	Ceftazidime	CAZ	30 µg	28 mm	Resistant
8	Ciprofloxacin	CIP	5 µg	39 mm	29 mm
9	Amikacin	AK	30 µg	28 mm	26 mm
10	Nitrofurantoin	NIT	300 µg	Resistant	18 mm
11	Netillin	NET	30 µg	31 mm	24 mm
12	Nalidixic acid	NA	30 µg	27 mm	25 mm
13	Streptomycin	S	10 µg	25 mm	28 mm
14	Sulphatriad	S3	300 µg	12 mm	Resistant
15	Tetracyline	TE	25 µg	20 mm	32 mm
16	Cephalothin	CEP	30 µg	Resistant	19 mm
17	Clindamycin	CD	2 µg	Resistant	29 mm
18	Erythromycin	E	15 µg	Resistant	22 mm
19	Oxacillin	OX	1 µg	Resistant	15 mm
20	Vancomycin	VA	30 µg	Resistant	22 mm
21	Ciprofloxacin	CIP	5 µg	40 mm	27 mm
22	Fosfomycin	FO	200 µg	32 mm	34 mm
23	Norfloxacin	NX	10 µg	40 mm	31 mm
24	Penicillin G	P	10 units	Resistant	13 mm
25	Levoflaxin	LE	5 µg	39 mm	29 mm
26	Ceftriaxone	CTR	30 µg	22 mm	22 mm
27	Chloramphenicol	C	30 µg	25 mm	27 mm
28	Rifampicin	R	5 µg	11 mm	15 mm
29	Kanamycin	K	5 µg	12 mm	20 mm

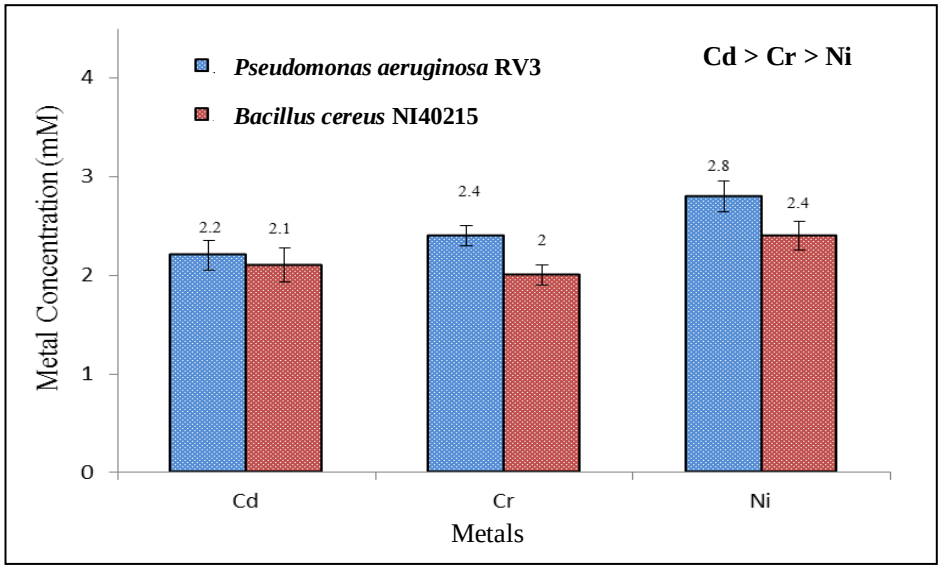

Figure 8: Determination of minimum inhibitory concentration (MIC) of heavy metals (Cd, Cr & Ni) in two bacterial strains: *Pseudomonas aeruginosa* RV3 and *Bacillus cereus* NI40215.

Table 4: Data represents the percentage change of mean values of growth rate as compared to untreated cells.

Percentage of Growth rate		
	***Pseudomonas aeruginosa* RV3 at 24 hr**	***Bacillus cereus* NI4 0215 at 12hr**
Cadmium		
Concentration	**Mean ± SD**	**Mean ± SD**
Control	100.00 ± 0.16	100.00 ± 0.46
0.5 mM	92 .96 ± 0.63 [a]	96.27 ± 1.05 [a]
2mM	63.57 ± 0.90 [a]	55.08 ± 0.69 [a]
Chromium		
Control	100.00 ± 0.16	100.00 ± 0.46
0.5 mM	80.70 ± 0.35 [a]	88.65 ± 0.37 [a]
2mM	59.38 ± 0.27 [a]	80.95 ± 1.10 [a]
Nickel		
Control	100.00 ± 0.16	100.00 ± 0.46
0.5 mM	93.57 ± 0.20 [a]	90.87 ± 2.97 [b]
2mM	82.13 ± 0.16 [a]	88.89 ± 0.78 [a]

Values are expressed as Mean of three independent observations. [a]$P \leq 0.001$ compared to control reaction; [b]$P \leq 0.01$ compared to control reaction; [c]$P \leq 0.05$ compared to control

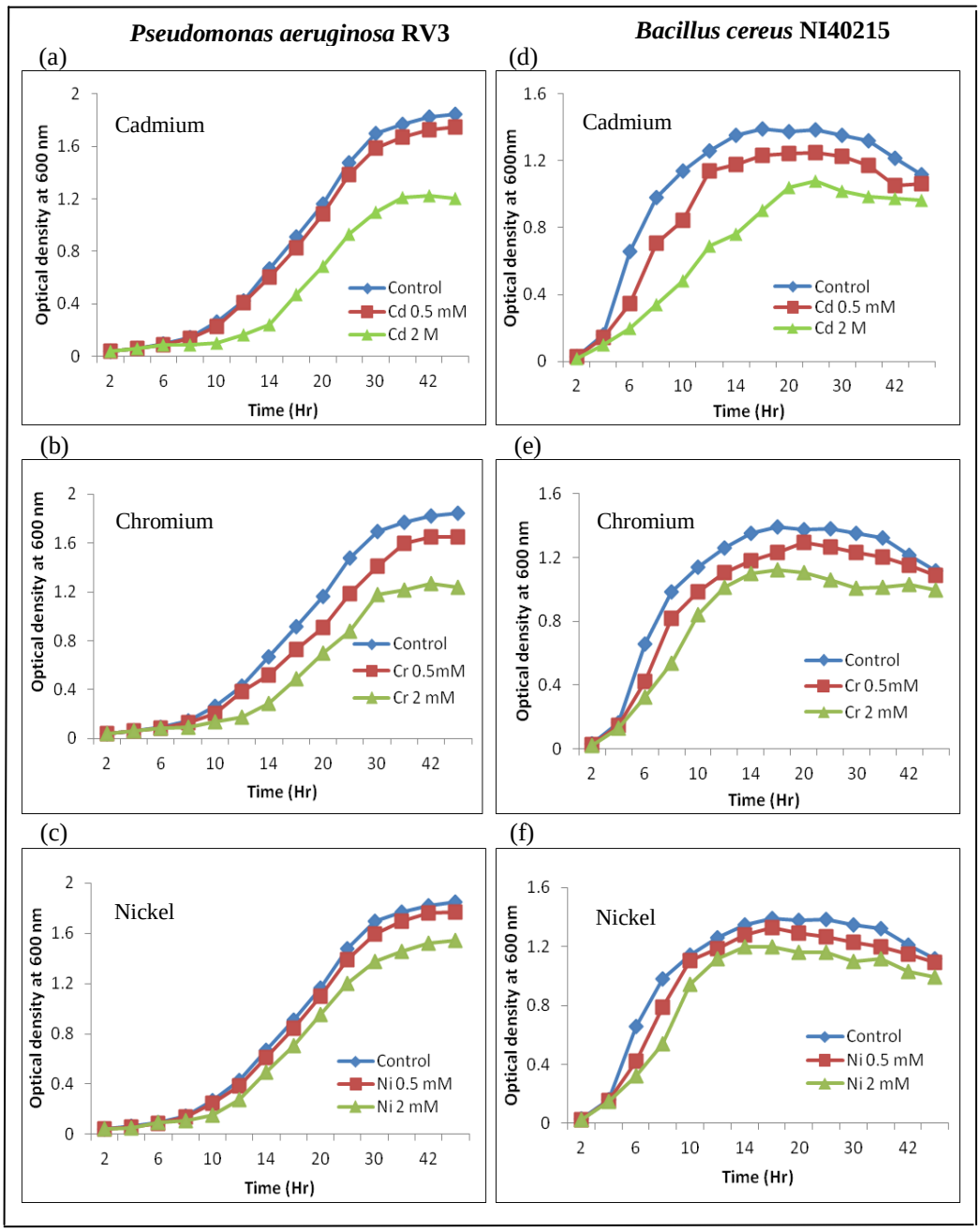

Figure 9: Effect of heavy metals on the growth of (a-c) *Pseudomonas aeruginosa* RV3 & (d-f) *Bacillus cereus* NI40215.

4.4.1 Effect of Metal ions (Cd, Cr & Ni) on Cellular damage: Response of GSH and Antioxidant Enzyme System in *Pseudomonas aeruginosa* RV3

Heavy metals are known to generate reactive oxygen species (ROS) leading to oxidative damage. The biological system utilizes both enzymatic and non-enzymatic mechanisms to mitigate ROS induced oxidative damage. Reduced glutathione (GSH) is one of the important components of non-enzymatic defense system which may prevent heavy metal toxicity by sequestration of the ROS, oxidizing it to glutathione (GSSG). In the present study, *Pseudomonas aeruginosa* RV3 treated with metals (Cd, Cr & Ni) showed significant decrease in the GSH levels at 6 h and 12 h for all metals as compared to untreated control (Figure 10 a-c). Lipid peroxidation is considered as a marker for membrane damage mediated through increased level of ROS. Here with increase in the doses of metals, significant increase in the peroxidation levels (expressed in terms of nano moles of malondialdehyde (MDA) formed per mg protein) was observed for both 6 h and 12 h (Figure 11 a-c). The increased level of peroxidation might be responsible for the decrease in the growth rate of the bacterial strain RV3 in the presence of metal (Figure 9 a-c & Table 4).

SOD, CAT, GPx and GR are important members of antioxidant enzyme system. Treatment of metals (Cd Cr & Ni) exhibited significant increase in the SOD activity in dose dependent manner at both 6 h and 12 h as compared to untreated control but decrease was observed at 12 h as compared with 6 h treated conditions (Figure 12 a-c). CAT activity in bacterial strain RV3 increased in dose dependent manner with the metal (Cd, Cr & Ni) treatment at 6 h and 12 h. In the Cd treated condition increased level of CAT activity was observed at 12 h as comparison with the 6 h treated condition (Figure 13a) but in the Cr and Ni treated cells decrease in the CAT activity was observed at 12 h particularly with the dose 0.5 mM as compared to 6h treated control (Figure 13b & 13c). GPx activity increased significantly in dose dependent manner with Cd and Ni treatment at 6 h and 12 h as compared to the untreated control

(Figure 14a & 14c). In case of Cr treated condition, significant increase in the GPx activity was observed as compared to untreated control at both the doses and time points, but dose dependent increase was only seen at 6 h. GR activity showed significant increase in dose dependent manner in the metal (Cd, Cr & Ni) treated conditions as compared to the untreated control (Figure 15 a-c).

4.4.2 Effect of Metal ions (Cd, Cr & Ni) on Cellular damage: Response of GSH and Antioxidant Enzyme Systems in *Bacillus cereus* NI40215

The role of GSH and antioxidant enzymes in response to heavy metal (Cd, Cr & Ni) was also studied in *Bacillus cereus* NI40215. *Bacillus* strain NI40215 exhibited significant dose dependent decrease in the GSH levels with all metals (Figure 10 d-f) as compared to the untreated control at 6 h and 12 h respectively. In contrast, lipid peroxidation increased significantly in dose dependent manner at both the time points as compared to the untreated control (Figure 11 d-f). This increase in the peroxidation levels might be responsible for the slower growth rate of the bacterial strain in presence of the metals (Figure 9 d-f & Table 4).

SOD and CAT are the first line of defense for neutralizing the ROS and peroxides generated in response to oxidative damage. Treatment of *Bacillus* strain NI40215 with the heavy metals (Cd, Cr & Ni) showed significant dose dependent increase in the SOD activity at 6 h and 12 h respectively as compared to untreated control (Figure 12 d-f). For the similar conditions CAT activity also increased in the dose dependent manner.

GPx activity also exhibited significant increase in dose dependent manner for the metal treated conditions as compared to untreated conditions (Figure 14 d-f). For Cd and Cr treated conditions, decline in the activity was seen at 12 h in comparison to the 6 h treated condition (Figure 14 d & e). GR activity showed significant dose dependent increase for all metal treated conditions at 6 h and 12 h respectively in comparison to untreated condition (Figure 15 d-f).

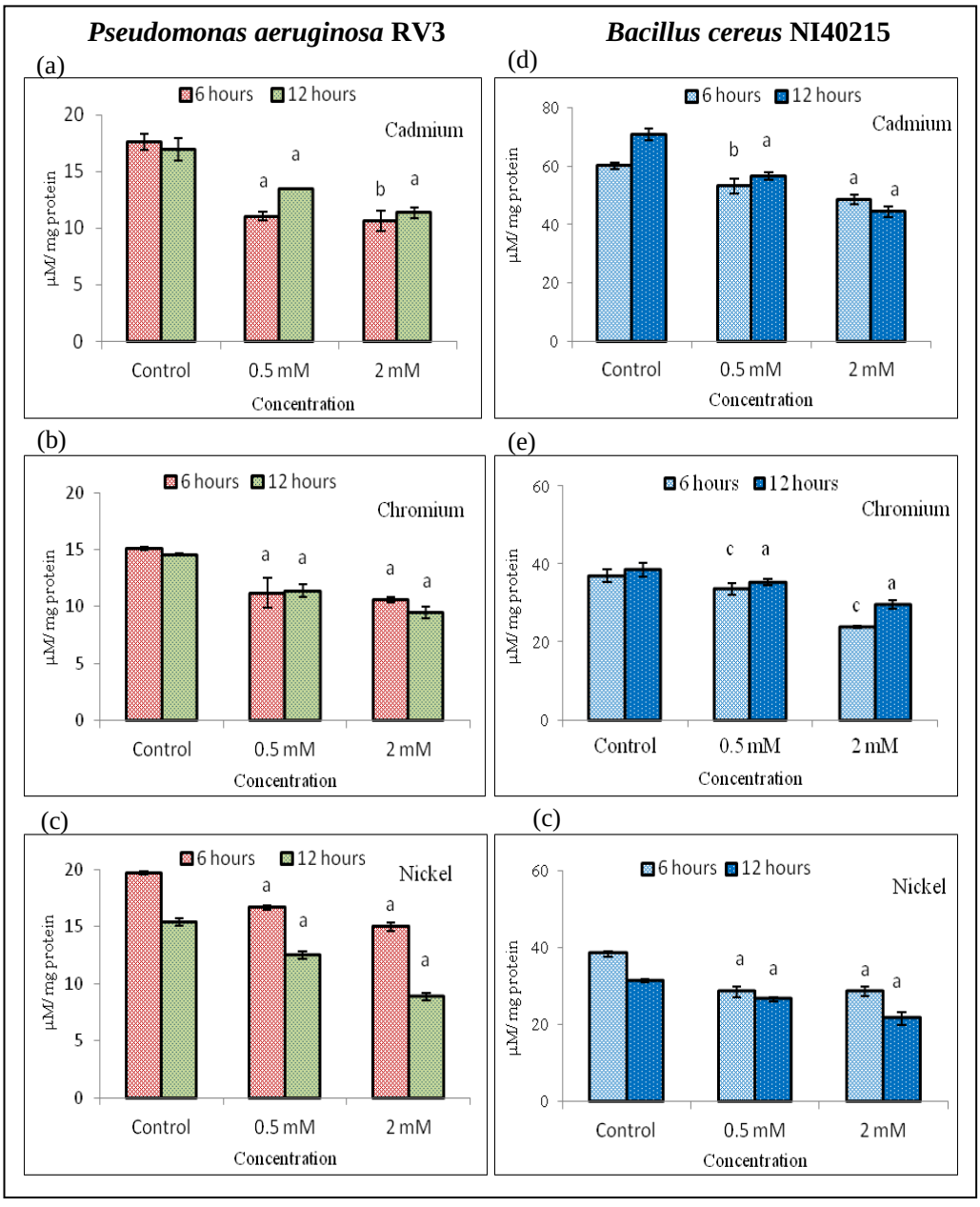

Figure 10: Effect of Heavy metals (Cd, Cr & Ni) on the reduced glutathione (GSH) level in the metal resistant bacterial strains.

Values are expressed as Mean of three independent observations. $^{a}P \leq 0.001$ compared to control reaction; $^{b}P \leq 0.01$ compared to control reaction; $^{c}P \leq 0.05$ compared to control reaction.

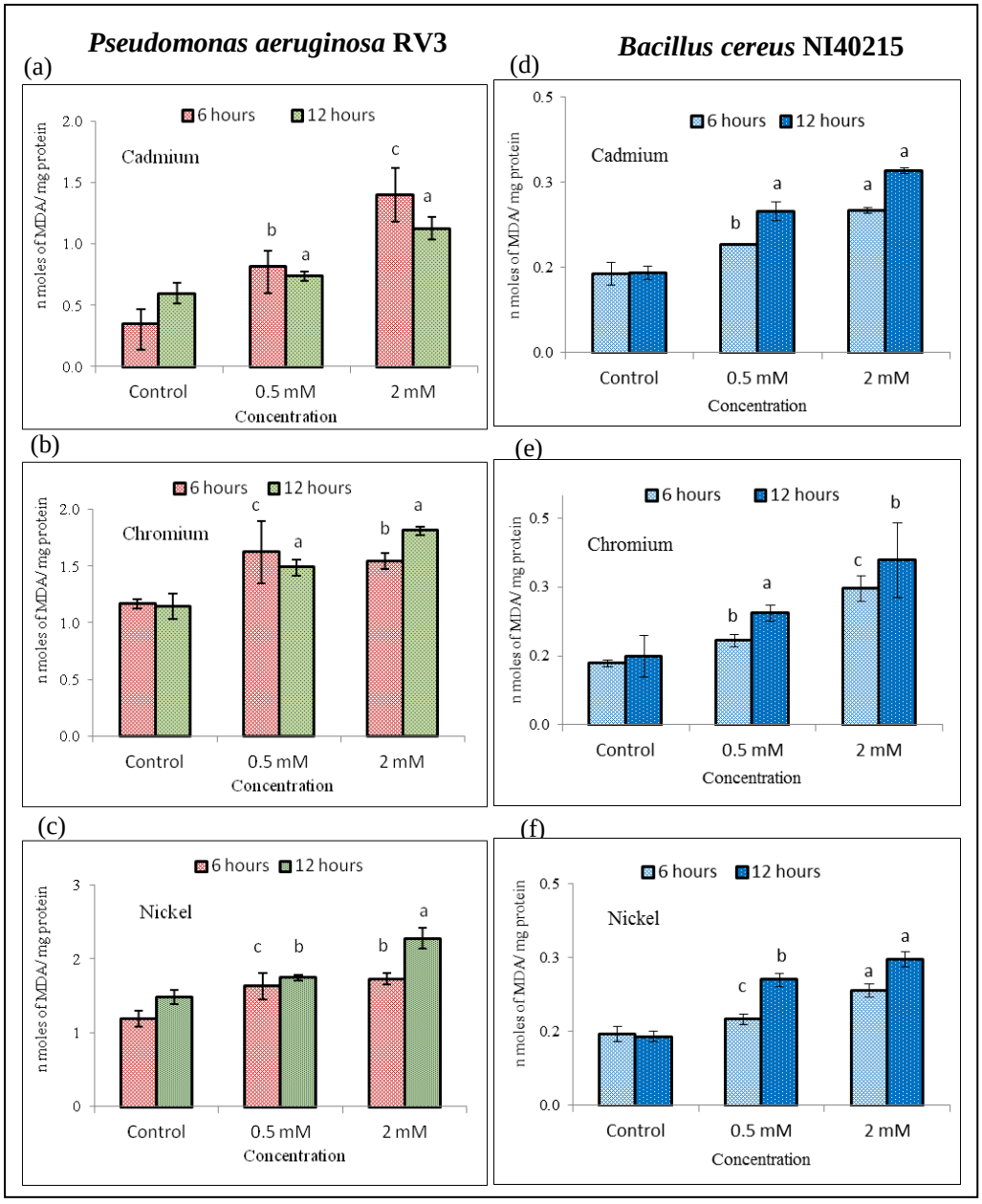

Figure 11: Effect of Heavy metals (Cd, Cr & Ni) on the lipid peroxidation (expressed as nmoles MDA/ mg of protein) in the metal resistant bacterial strains.

Values are expressed as Mean of three independent observations. $^{a}P \leq 0.001$ compared to control reaction; $^{b}P \leq 0.01$ compared to control reaction; $^{c}P \leq 0.05$ compared to control reaction.

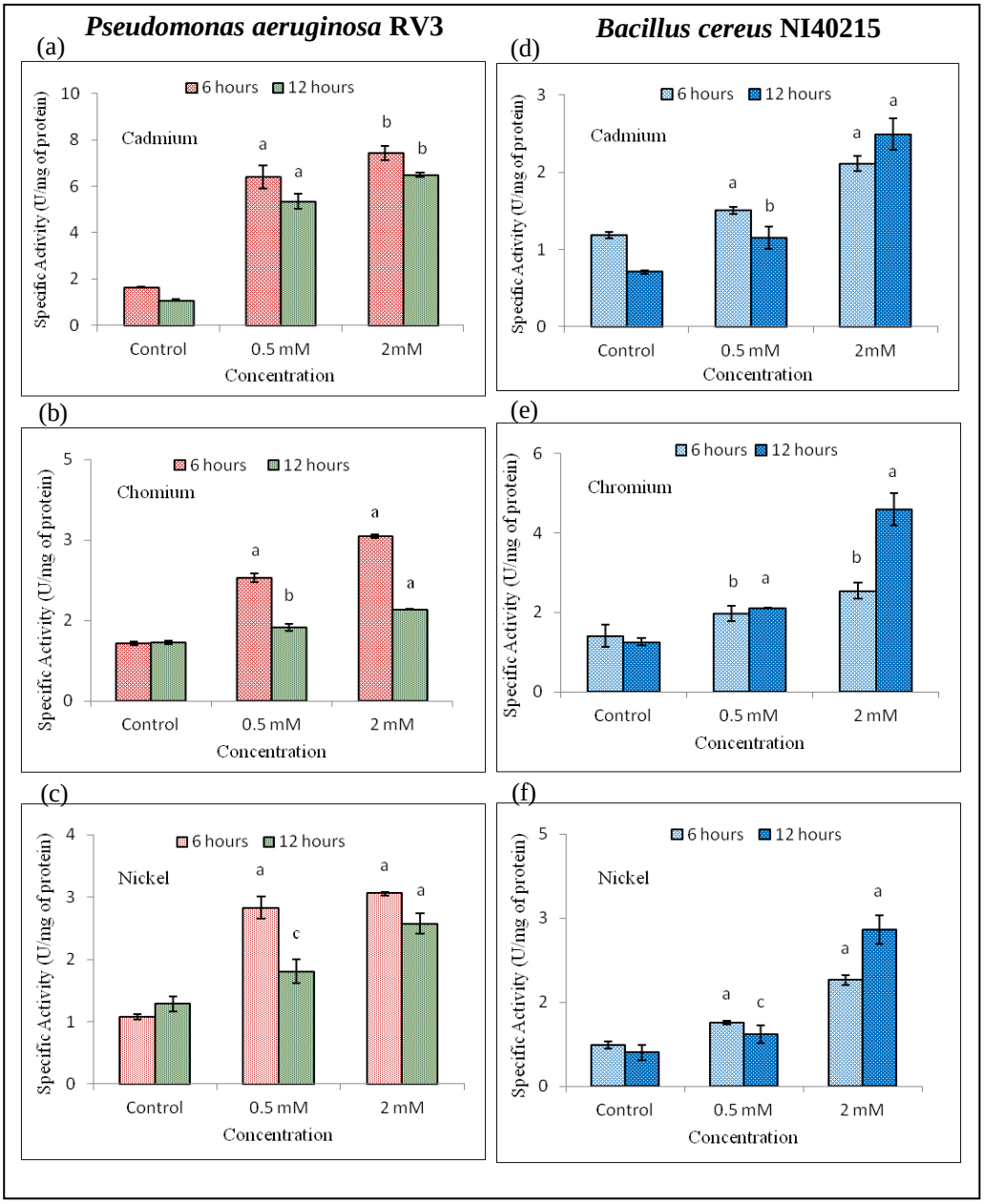

Figure 12: Effect of Heavy metals (Cd, Cr & Ni) on the specific activity of superoxide dismutase (SOD) in the metal resistant bacterial strains.

Values are expressed as Mean of three independent observations. $^{a}P \leq 0.001$ compared to control reaction; $^{b}P \leq 0.01$ compared to control reaction; $^{c}P \leq 0.05$ compared to control reaction.

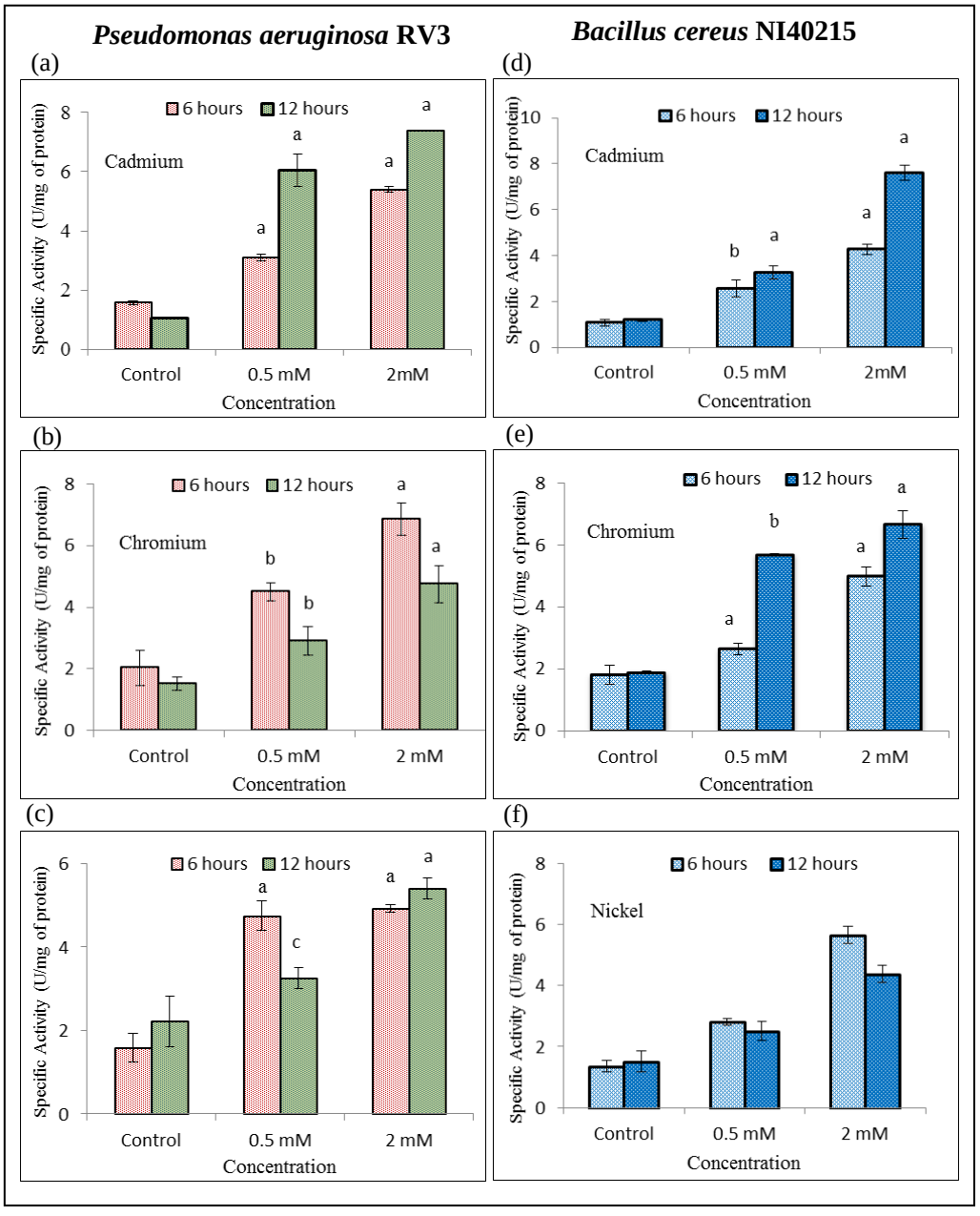

Figure 13: Effect of Heavy metals (Cd, Cr & Ni) on the specific activity of Catalase (CAT) in the metal resistant bacterial strains.

Values are expressed as Mean of three independent observations. $^{a}P \leq 0.001$ compared to control reaction; $^{b}P \leq 0.01$ compared to control reaction; $^{c}P \leq 0.05$ compared to control reaction.

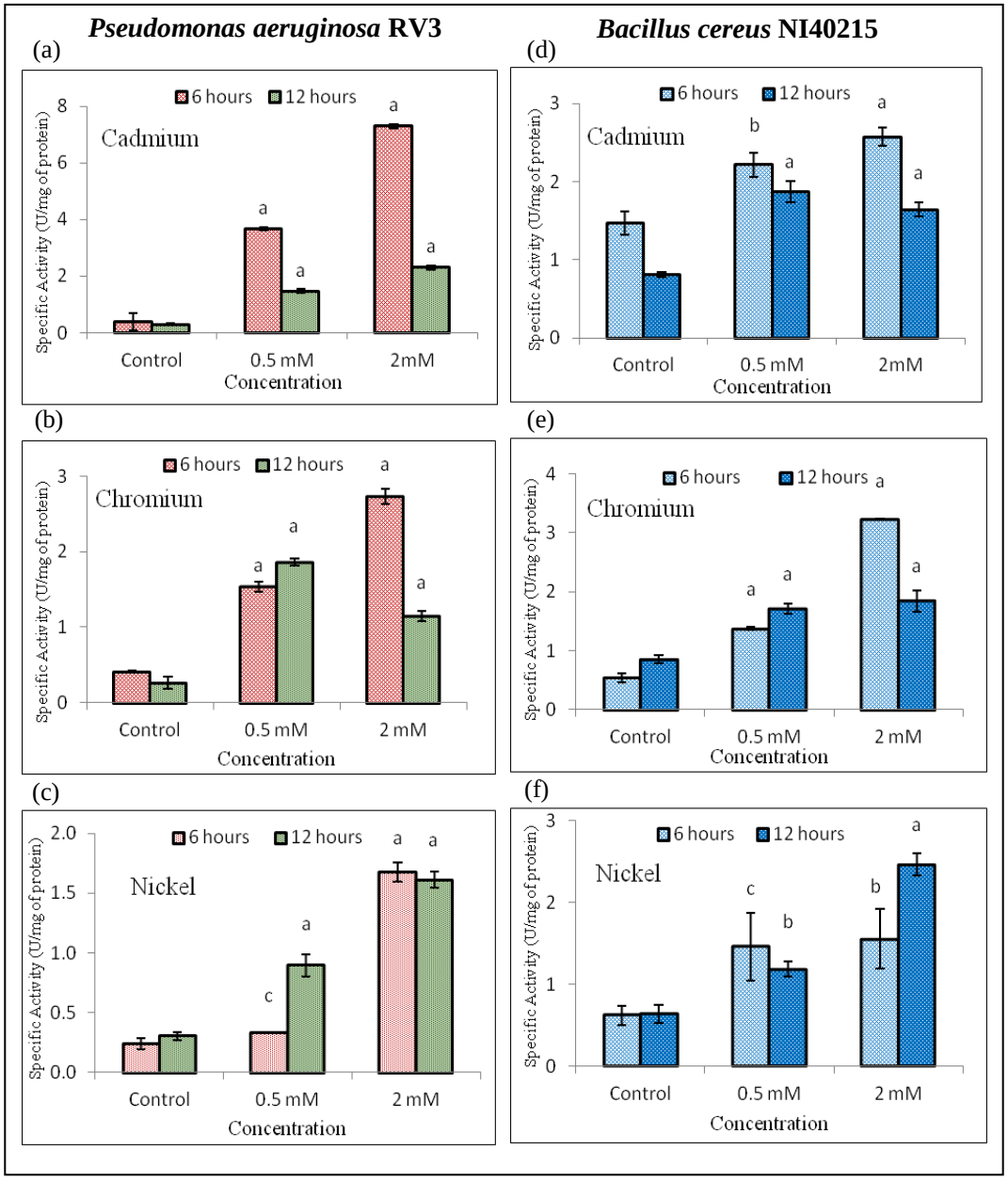

Figure 14: Effect of Heavy metals (Cd, Cr & Ni) on the specific activity of Glutathione peroxidase (GPx) in the metal resistant bacterial strains.

Values are expressed as Mean of three independent observations. $^{a}P \leq 0.001$ compared to control reaction; $^{b}P \leq 0.01$ compared to control reaction; $^{c}P \leq 0.05$ compared to control reaction.

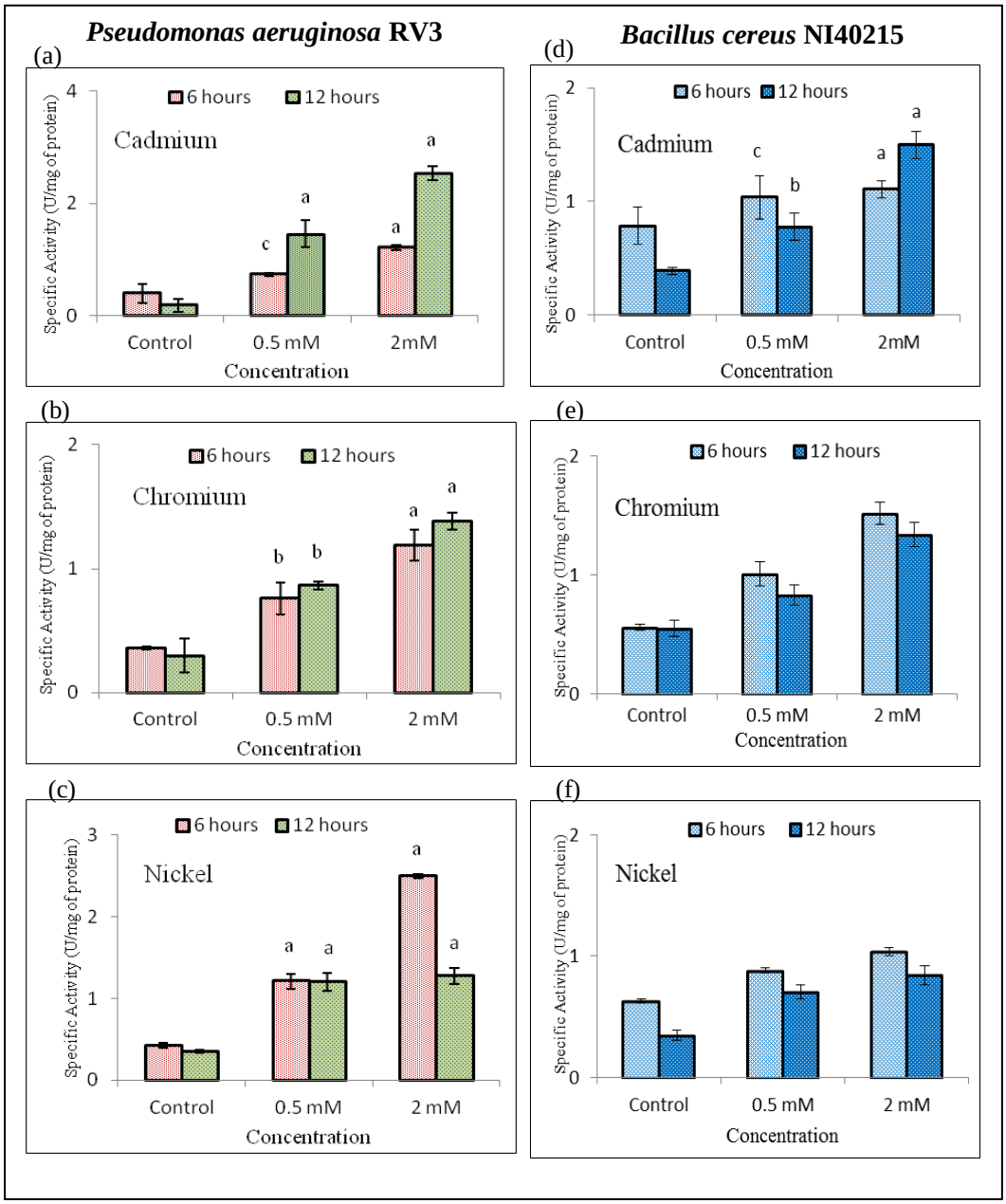

Figure 15: Effect of Heavy metals (Cd, Cr & Ni) on the specific activity of Glutathione reductase (GR) in the metal resistant bacterial strains.

Values are expressed as Mean of three independent observations. $^{a}P \leq 0.001$ compared to control reaction; $^{b}P \leq 0.01$ compared to control reaction; $^{c}P \leq 0.05$ compared to control reaction.

4.5.1 Biophysical analysis of Metal-Microbe interactions in *Pseudomonas aeruginosa* RV3

Scanning electron microscopy was used to study the morphological changes in the bacterial strains. In the present study, we observed changes in the morphology of *Pseudomonas aeruginosa* RV3 in response to metals (Cd, Cr & Ni). In the untreated conditions bacterial strain was rod shaped and elongated, and there were no peaks of metals (Cd, Cr & Ni) in their respective untreated control while in the treated conditions morphological changes are observed with decrease in surface/volume ratio (Figure 16 & Table 5). Bacterial strain became small with irregular edges on cell wall and EDX analysis showed metal peaks for Cd, Cr & Ni in their respective treated conditions. Interestingly we observed the increase in P (Phosphorus) element in the treated conditions particularly for Cd & Cr as compared to untreated control, but with increase in the treatment doses from 0.5 mM to 2 mM, it showed decrease in P element (Figure 17). For similar conditions in Cd and Ni P elements decreased with the increase in the doses of metals, but in case of Cr it increased (Figure 17).

FTIR spectra for the control (untreated) and treated bacterial strain were performed to get a qualitative analysis of the role of cellular functional groups involved in metal binding by the bacteria. The functional groups present on the bacterial cell wall are responsible for absorption of metals (Cd, Cr & Ni) due to non-specific binding of metal ions with them. The spectral analysis of control and metal (Cd, Cr & Ni) treated *Pseudomonas aeruginosa* RV3 indicated change in wave number in the spectral range 3200-3600 cm^{-1} (Stretching of N-H bond of amino and hydroxyl group). The appearance of new peaks in this region suggests strong interaction of N-H bond of amino groups and hydroxyl group with the metal ions (Cd, Cr & Ni) (Figure 18, Table 6).

The changes in the wave number was also observed in the spectral range 2000-2400 cm^{-1} (C, N, O) and 1500–1600 cm^{-1} (C-C, C-O, C-N, -COOH group) for all the metals. The peaks in the range of 1300 – 1067 cm^{-1} are attributable to the presence of carboxyl and phosphate groups and peaks in range of 700 – 1000 cm^{-1} to the presence of aromatic –CH stretching were also found to be shifted. FTIR studies showed that functional groups like bonded –OH, aliphatic C-H, C-O, C-N, -COOH and P=O & P-O are involved in Cd, Cr and Ni adsorption.

Transmission electron microscopy (TEM) was used to investigate the intracellular localization of accumulated metals within the bacterial strain *Pseudomonas aeruginosa* RV3. The untreated control represented relatively diffused cell boundary and homogeneous cytoplasm with few electron dense granules and in contrast, metal treated strain presented a dark electron opaque ring throughout the cell periphery indicating the preferential metal deposition in cell wall, periplasmic membrane and cytoplasm components. TEM images indicates the accumulation of metals (Cd, Cr & Ni) in the treated strain as compared to the untreated control (Figure 19).

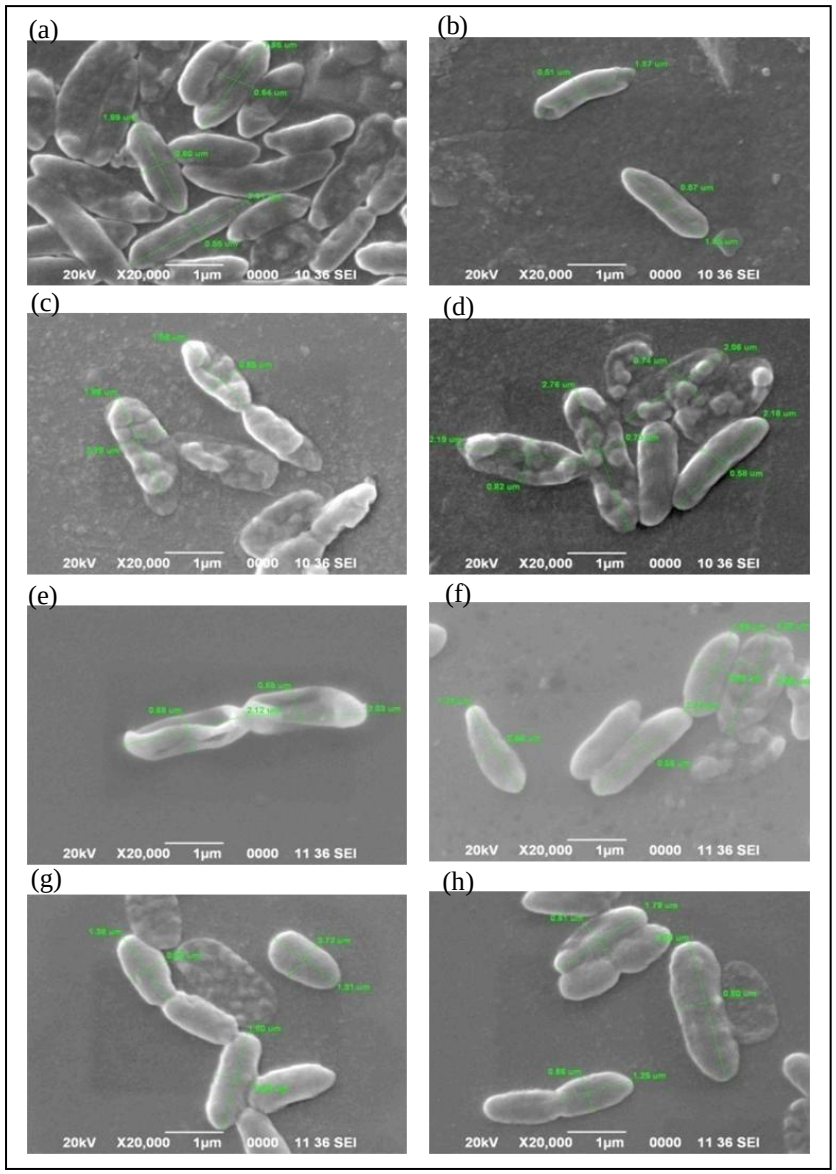

Figure 16: Scanning electron micrograph of *Pseudomonas aeroginosa* RV3 (a) & (b) Control cells (without exposure to metal ions) (c) & (d) cells grown in presence of Cd 0.5 mM & 2 mM ; (e) & (f) in presence of Cr 0.5 mM & 2 mM ; (g) & (h) in presence of Ni 0.5 mM & 2 mM.

Table 5: Effect of heavy metal (Cd, Cr, Ni) on the dimension metal resistant *Pseudomonas aeruginosa* RV3

Conc. in mM		Height (µm)	Radius (µm)	Surface Area (μm^2)	Volume (μm^3)	Surface/ Volume
Control		2.00 ± 0.19	0.30 ± 0.02	2.17	0.57	3.81
Cd	**0.5**	1.78 ± 0.13	0.32 ± 0.05	2.11	0.57	3.70
	2.0	2.30 ± 0.27	0.36 ± 0.04	3.01	0.94	3.20
Cr	**0.5**	2.11 ± 0.07	0.35 ± 0.03	2.71	0.81	3.35
	2.0	1.93 ± 0.22	0.33 ± 0.06	2.35	0.66	3.56
Ni	**0.5**	1.38 ± 0.25	0.34 ± 0.02	1.84	0.50	3.68
	2.0	1.92 ± 0.36	0.34 ± 0.06	2.42	0.70	3.46

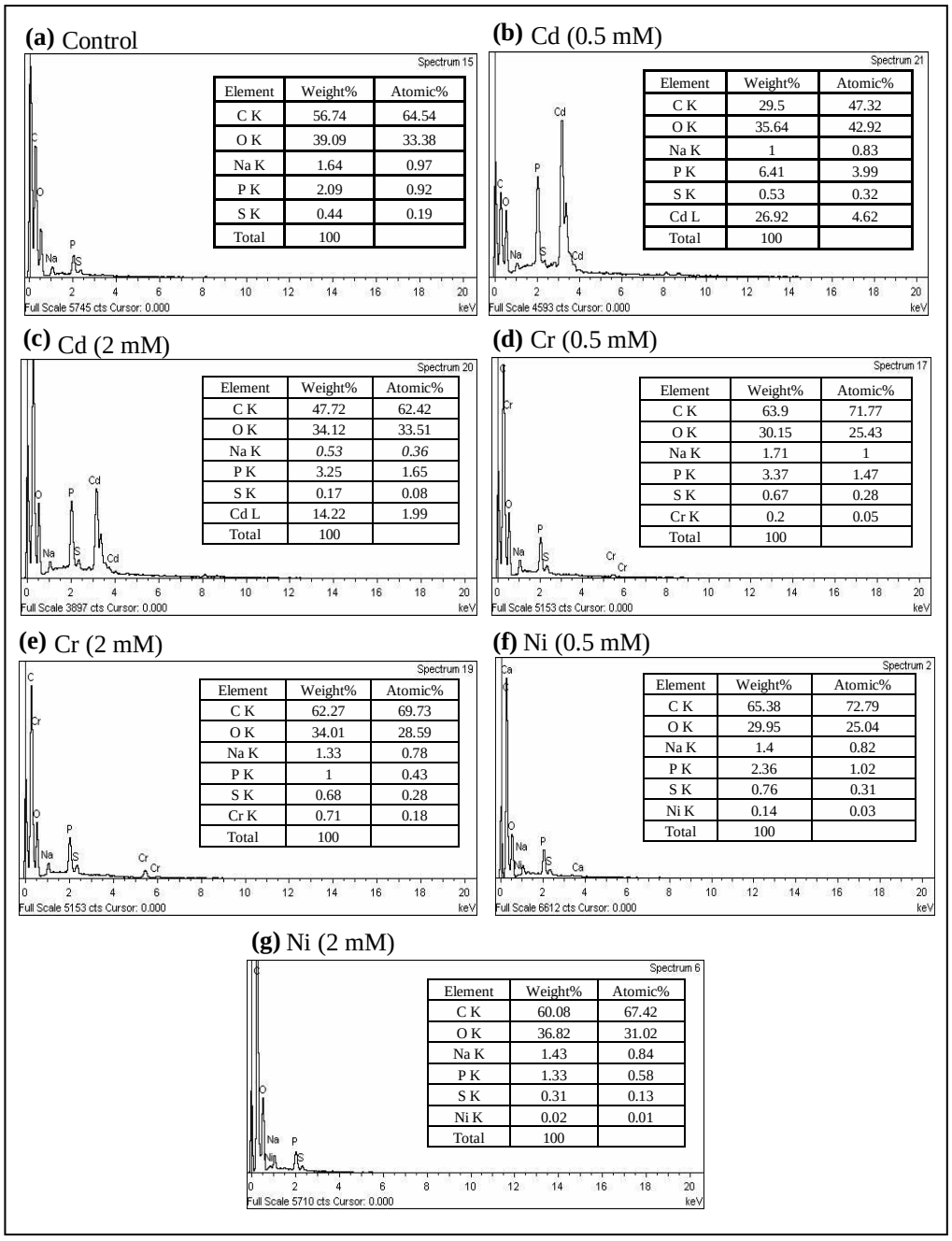

Figure 17: Energy dispersive X-Ray spectra of *Pseudomonas aeruginosa* RV3 (a) control, (b) & (c) treated with Cd 0.5 mM & 2 mM, (d) & (e) treated with Cr 0.5 mM & 2 mM, (f) & (g) treated with Ni 0.5 mM & 2 mM.

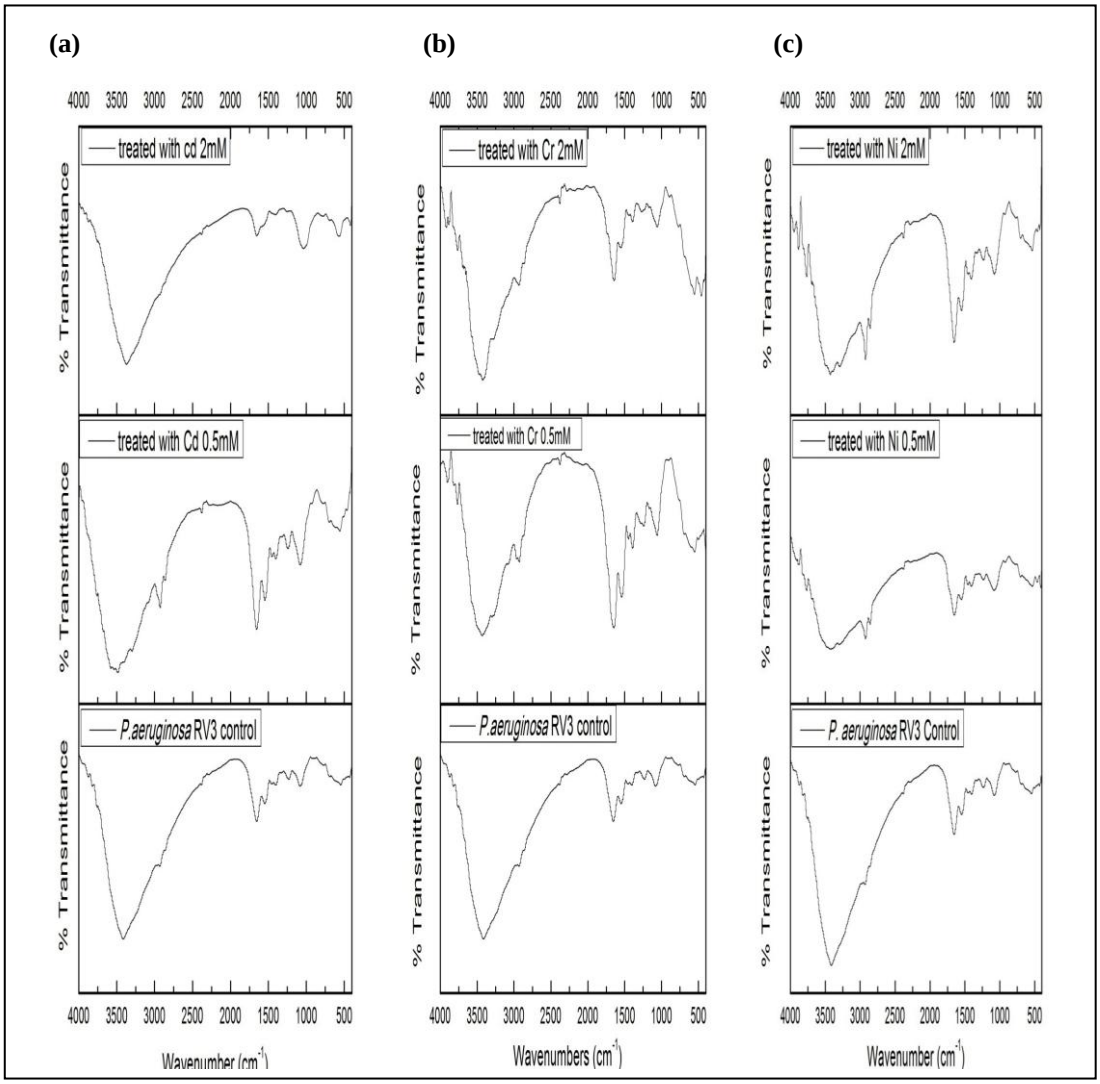

Figure 18: FTIR spectra of *Pseudomonas aeruginosa* RV3 treated with (a) Cd 2 mM, 0.5 mM & Control, (b) Cr 2 mM, 0.5 mM & Control, (c) Ni 2 mM, 0.5 mM & Control.

Table 6: The FTIR spectral characteristics of *Pseudomonas aeruginosa* RV3 treated with different metal ions.

Sl No	Control	Cd 0.5mM	Cd 2mM	Cr 0.5mM	Cr 2mM	Ni 0.5mM	Ni 2mM	Reference
1	3423	3477	3368	3427	3416	3437	3427	(3200-3600) cm^{-1} Stretching of N-H bond of amino group along with O-H of hydroxyl groups
2	-	3293	-	3276	3266	3293	3293	
3	2935	2924	-	2932	2922	2925	2925	(2900-3000) cm^{-1} C-H bond of CH_2 & CH_3 groups, Asymmetric stretching
4	2858	2849	-	2861	2841	2853	2842	
5	2390	2370	2382	2375	2375	2382	2382	(2000 -2400)cm^{-1} C, N, O
6	1654	1654	1654	1647	1638	1654	1654	(1600-1900) cm^{-1} C=O
7	1547	1545	-	1537	1547	1551	1551	(1000-1600)cm^{-1} C-C, C-O, C-N,-COOH group. P=O & P-O of $C-PO_3^{2-}$ moiety
8	1459	1448	-	1456	1446	1454	1454	
9	1408	1393	1403	1398	1398	1408	1408	
10	1230	1240	1230	1233	-	1233	1233	
11	1077	1077	1038	1061	1061	1070	1070	
12	774	774	784	-	777	803	782	(700-1000) cm^{-1} CH-CH groups

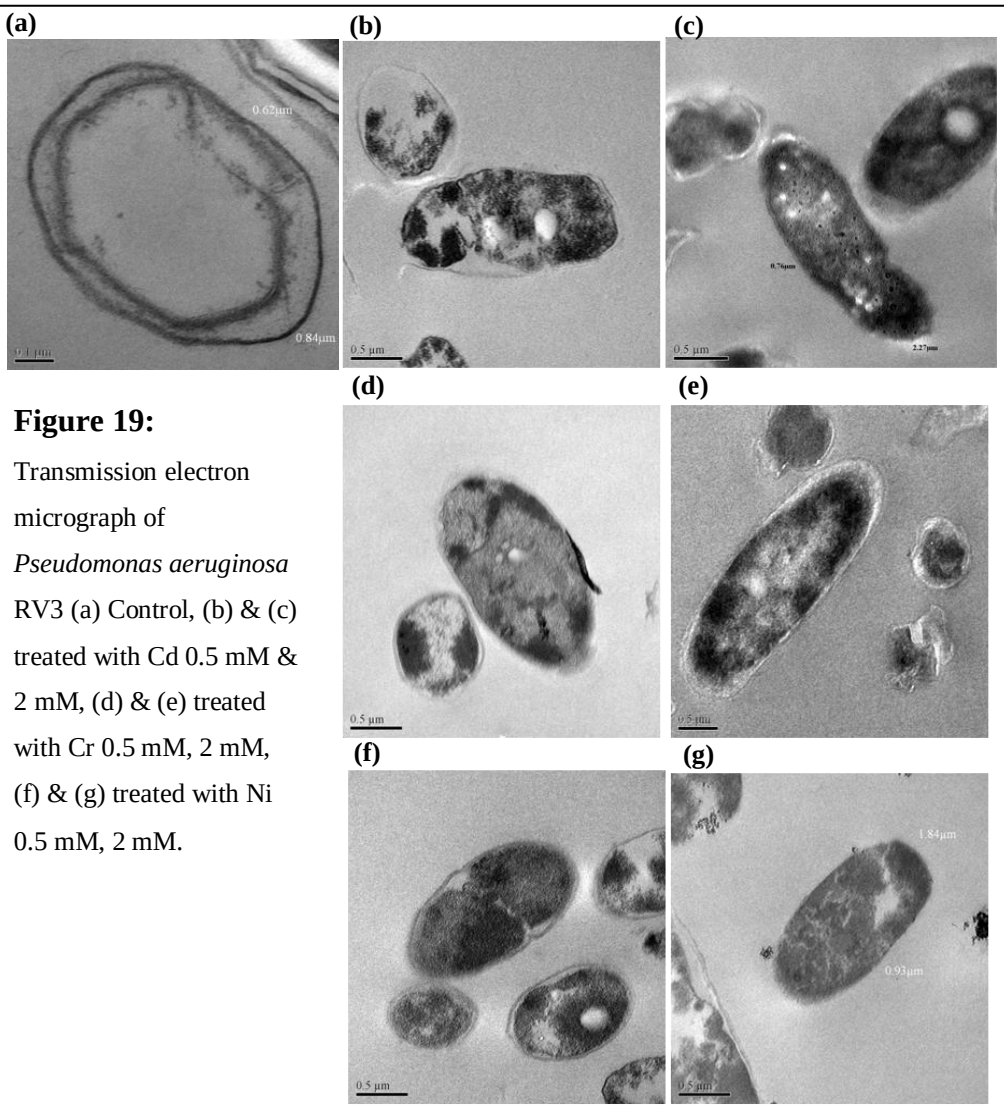

Figure 19:

Transmission electron micrograph of *Pseudomonas aeruginosa* RV3 (a) Control, (b) & (c) treated with Cd 0.5 mM & 2 mM, (d) & (e) treated with Cr 0.5 mM, 2 mM, (f) & (g) treated with Ni 0.5 mM, 2 mM.

4.5.2 Biophysical analysis of Metal-Microbe interactions in *Bacillus cereus* NI40215

Scanning electron microscopy (SEM) of *Bacillus cereus* NI40215 showed rod shaped and smooth surface morphology with average surface to volume (S/V) ratio of 3.07 (Figure 20 & Table 7). When the strain NI40215 was exposed separately to different heavy metals (Cd, Cr & Ni) change in the surface morphology was observed with decrease in the S/V ratio (Table 7). The surface morphology changed to irregular/rough with the exposure to metals and was more distinct at 2 mM concentration of Cd, Cr and Ni (Figure 20). Interestingly, under all metal stress conditions dividing cells were observed. EDX analysis of the NI40215 strain showed the metal peaks in the metal treated cells as compared to the untreated cells (Figure 21). Also increase in the level of phosphorus (P) was observed particularly for Cd and Cr treated conditions. EDX analysis showed decrease in the metal with increase in the dose for Cd and Ni but in case of chromium increase was observed (Figure 21). This shows that bacterial strain responds differently with different metals suggesting metal dependent mechanism of interactions.

The FITR spectra of metal treated and untreated *Bacillus cereus* NI40215 biomass in the range of 400 – 4000 cm^{-1} were taken to confirm the presence of functional groups that are responsible for the absorption process (Figure 22 & Table 8). The control (untreated) biomass showed number of absorption peaks, reflecting the complex nature of the biomass. The shift in the peak positions in the range of 3200 – 3600 cm^{-1} indicative of strong interactions with the N-H bond of amino group and O-H of hydroxyl groups of the proteins. Interestingly, in the metal treated biomass few peaks disappeared in this region (Table 8).

The changes in the absorption peaks in the range of 2900 – 3000 cm^{-1} (C-H bond of CH_2 & CH_3 groups), 2000 – 2400 cm^{-1} (C, N, O), 1600 – 1900 cm^{-1} (C=O), 1000 -1600 cm^{-1} (C-C, C-O, C-N, -COOH groups; P=O & P-O of C-PO_3 moiety) and 700 – 1000 cm^{-1} (CH-CH groups) suggests possible complex interaction of metals (Cd, Cr & Ni) in the NI40215 strain (Table 8). FTIR studies showed complex interaction of metals (Cd, Cr & Ni) within the wide range of the spectra involving functional groups present on the bacterial biomass such as bonded –OH, aliphatic C-H, secondary amines, carboxyl, carbonyl, phosphonate and phosphate diester groups.

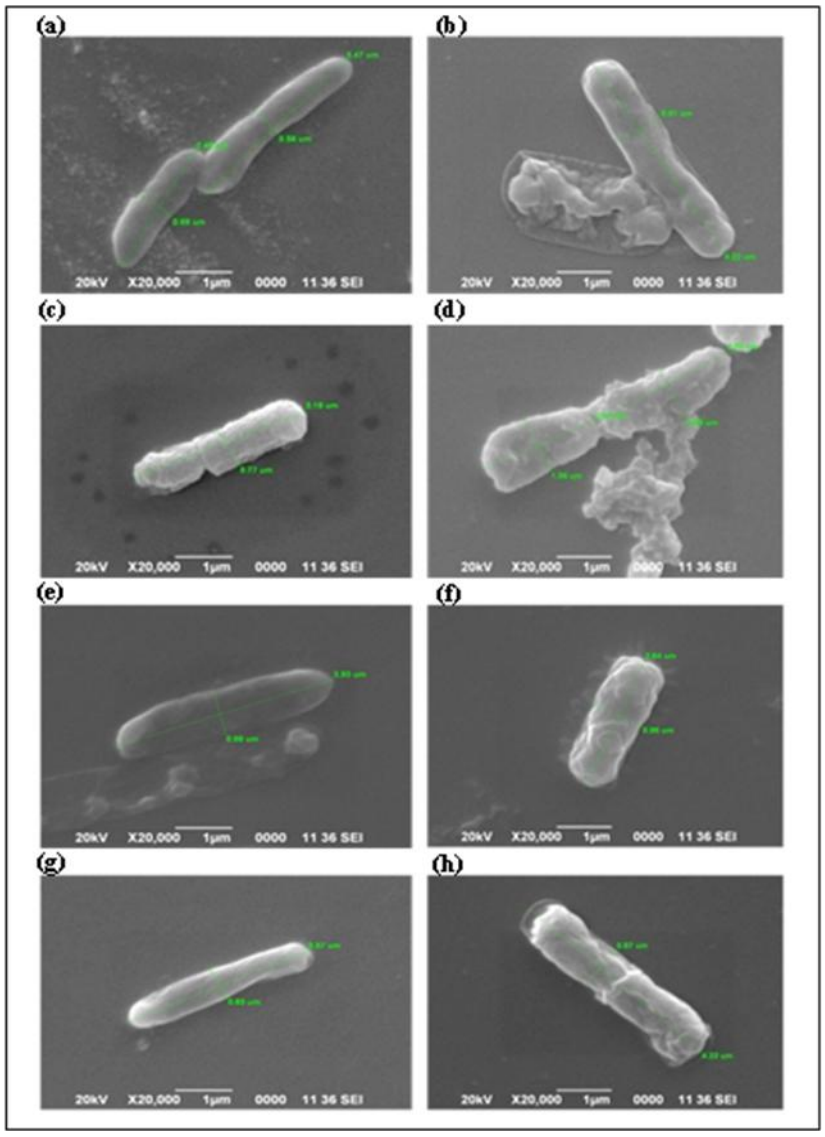

Figure 20: Scanning electron micrograph of *Bacillus cereus* NI49215 (a) & (b) Control cells (without exposure to metal ions); (c) & (d) cells grown in presence of Cd 0.5mM & 2mM ; (e) & (f) in presence of Cr 0.5mM & 2mM ; (g) & (h) in presence of Ni 0.5mM & 2mM.

Table 7: Effect of heavy metal (Cd, Cr, Ni) on the dimension of metal resistant *Bacillus cereus* NI40215

Conc. in mM		Height (µm)	Radius (µm)	Surface Area (μm^2)	Volume (μm^3)	Surface/ Volume
	Control	3.49 ± 0.75	0.36 ± 0.08	4.36	1.42	3.07
Cd	**0.5**	2.60 ± 0.34	0.50 ± 0.07	4.87	2.04	2.39
	2.0	2.49 ± 0.37	0.49 ± 0.10	4.56	1.88	2.43
Cr	**0.5**	3.54 ± 0.25	0.34 ± 0.08	4.15	1.29	3.22
	2.0	2.68 ± 0.25	0.47 ± 0.02	4.65	1.86	2.50
Ni	**0.5**	3.49 ± 0.09	0.31 ± 0.04	3.70	1.05	3.52
	2.0	3.71 ± 0.49	0.38 ± 0.07	4.89	1.68	2.91

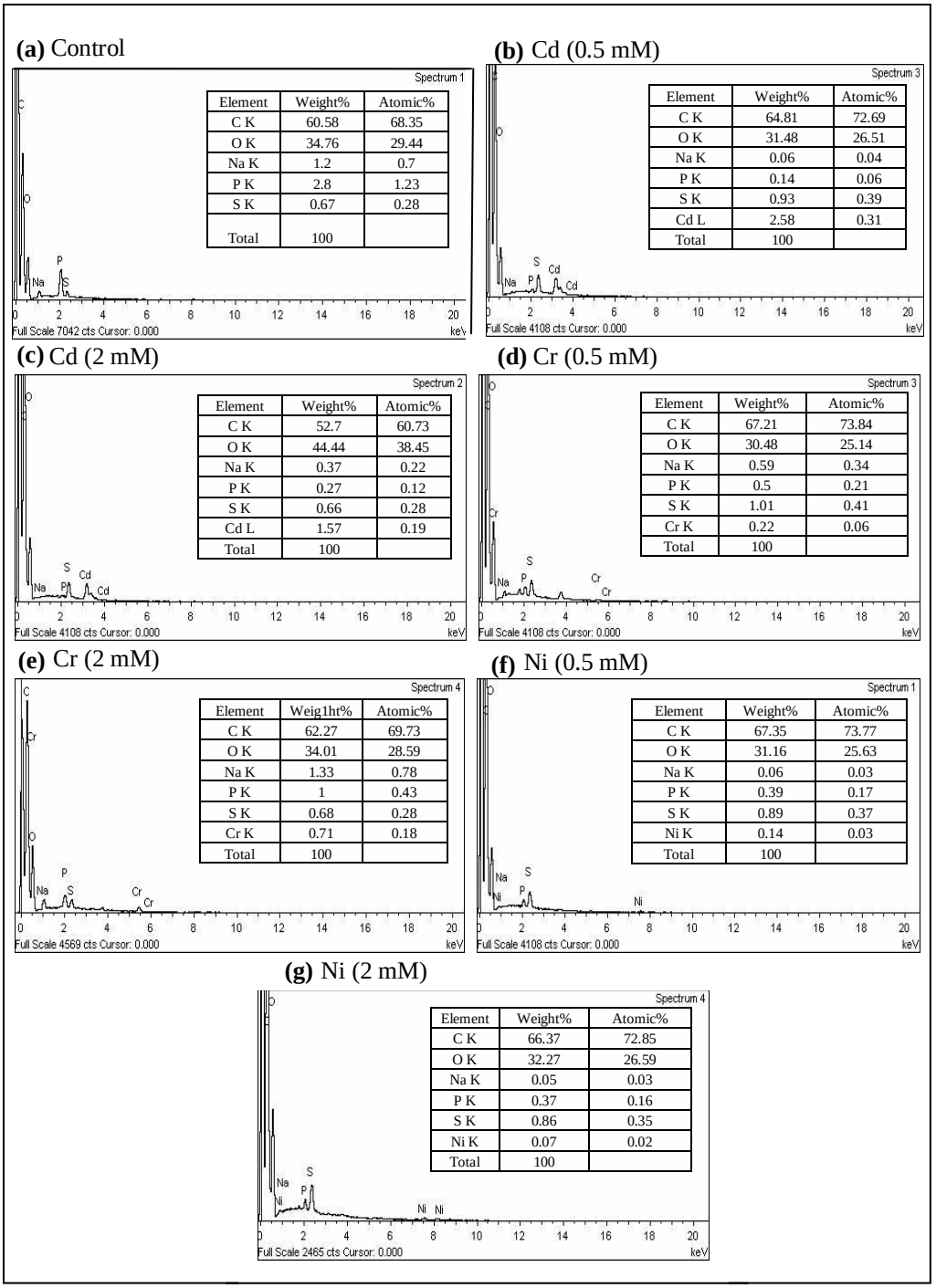

Figure 21: Energy dispersive X-Ray spectra of *Bacillus cereus* NI40215 (a) control, (b) & (c) treated with Cd 0.5 mM & 2 mM, (d) & (e) treated with Cr 0.5 mM & 2 mM, (f) & (g) treated with Ni 0.5 mM & 2 mM.

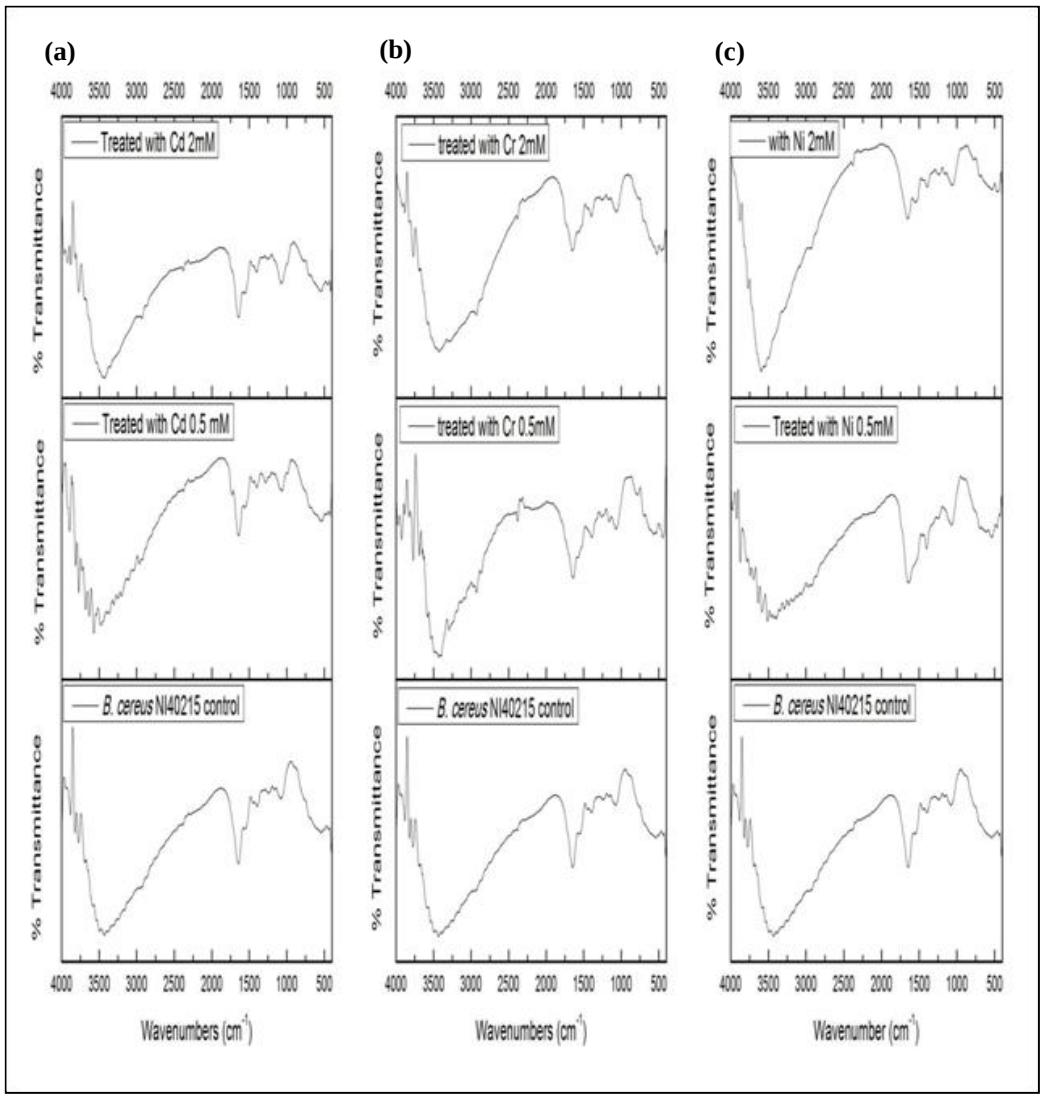

Figure 22: FTIR spectra of *Bacillus cereus* NI40215 treated with (a) Cd 2 mM, 0.5 mM & Control, (b) Cr 2 mM, 0.5 mM & Control, (c) Ni 2 mM, 0.5 mM & Control.

Table 8: The FTIR spectral characteristics of *Bacillus cereus* NI40215 treated with different metal ions.

Sl No	Control	Cd 0.5 mM	Cd 2 mM	Cr 0.5 mM	Cr 2 mM	Ni 0.5 mM	Ni 2 mM	Reference
1	3442	3477	3432	3439	3421	3458	3578	(3200-3600) cm^{-1} Stretching of N-H bond of amino group along with O-H of hydroxyl groups
2	3384	3365	3355	3301	3306	-	-	
3	3252	-	-	3286	3292	3288	-	
4	2960	2957	2927	2930	2930	2928	2938	(2900-3000) cm^{-1} C-H bond of CH_2 & CH_3 groups, Asymmetric stretching
5	2394	2374	2385	2380	2380	-	2382	(200 -2400) cm^{-1} C, N, O
6	1652	1643	1633	1640	1646	1644	1652	(1600-1900) cm^{-1} C=O
7	1556	1553	1564	-	-	-	1547	
8	1456	1456	1456	-	-	1449	-	(1000-1600)cm^{-1} C-C, C-O, C-N,-COOH group P=O & P-O of C-PO_3^{2-} moiety
9	1238	1286	1248	1248	1248	1233	1233	
10	1168	1179	-	1168	1158	-	1163	
11	1080	1070	1080	1069	1069	1080	1059	

4.6.1 Bio-sorption of Heavy metals in the *Pseudomonas aeruginosa* RV3 and *Bacillus cereus* NI40215

The amount of metal absorbed by the bacterial cells was detected by the Atomic Absorption spectroscopy (AAS). The concentration of metals taken up by the bacterial strains incubated with the metals for 24 h (a) *Pseudomonas aeruginosa* RV3 were Cd (0.1, 0.5 mM) 0.171 and 0.434 mg/gm of dry biomass; Cr (0.1, 0.5 mM) 0.031 and 0.080 mg/gm of dry biomass; Ni (0.1, 0.5 mM) 0.032 and 0.161 mg/gm of dry biomass (Figure 23 & Table 9) (b) *Bacillus cereus* NI40215 were Cd (0.1, 0.5 mM) 0.115 and 0.974 mg/gm of dry biomass; Cr (0.1, 0.5 mM) 0.050 and 0.531 mg/gm of dry biomass; Ni (0.1, 0.5 mM) 0.017 and 0.179 mg/gm of dry biomass (Figure 24 & Table 10). Using AAS the order of metal absorption in *Pseudomonas* strain was Cd > Ni > Cr and in case of *Bacillus* strain, the order of metal absorption was Cd > Cr > Ni. Interestingly *Bacillus* strain showed higher levels of metal absorption for all metals Cd, Cr and Ni in comparison to the *Pseudomonas* strain.

Bio-accumulation data were further confirmed with more sensitive method by inductively coupled plasma-optical emission spectrometry (ICP-OES). ICP-OES analysis also showed increase in the metal accumulation in the bacterial strains with increase in the concentration of metals but the amount of metals detected by this method were of much higher concentration as compared to AAS, this might be due to difference in the sensitivity of the instruments. Similar trend in the order of metal accumulation was observed for both the strains (Figure 25 & Table 11; Figure 26 & Table 12). ICP-OES analysis also showed higher levels of metal accumulation in the *Bacillus* strain as compared with *Pseudomonas* strain.

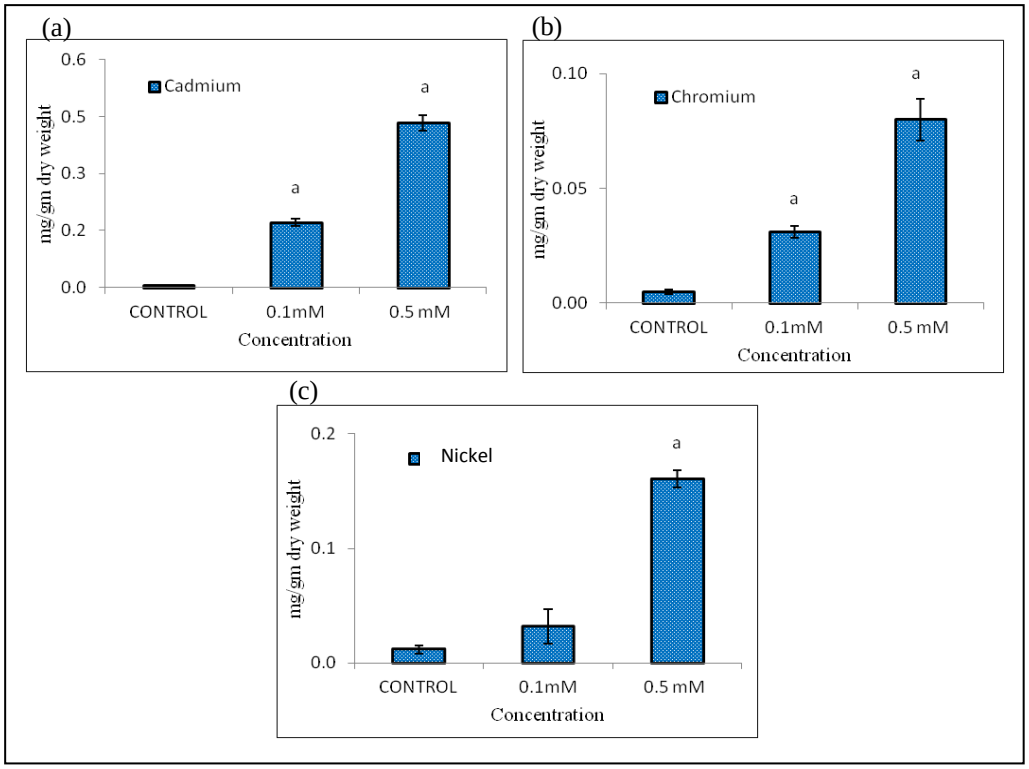

Figure 23: Atomic absorption spectroscopic analysis (AAS) of metals (Cd, Cr, Ni) in the dry biomass of metal resistant *Pseudomonas aeruginosa* RV3.

Values are expressed as Mean of three independent observations. $^{a}P \leq 0.001$ compared to control reaction; $^{b}P \leq 0.01$ compared to control reaction; $^{c}P \leq 0.05$ compared to control reaction.

Table 9: AAS data of metal ions in the dry biomass of metal resistant *Pseudomonas aeruginosa* RV3

Conc.	Cd Mean ± SD	Cr Mean ± SD	Ni Mean ± SD
CONTROL	0.005 ± 0.001	0.005 ± 0.001	0.012 ± 0.004
0.1mM	0.171 ± 0.008 [a]	0.031 ± 0.002 [a]	0.032 ± 0.015
0.5 mM	0.434 ± 0.021 [a]	0.080 ± 0.009 [a]	0.161 ± 0.007 [a]

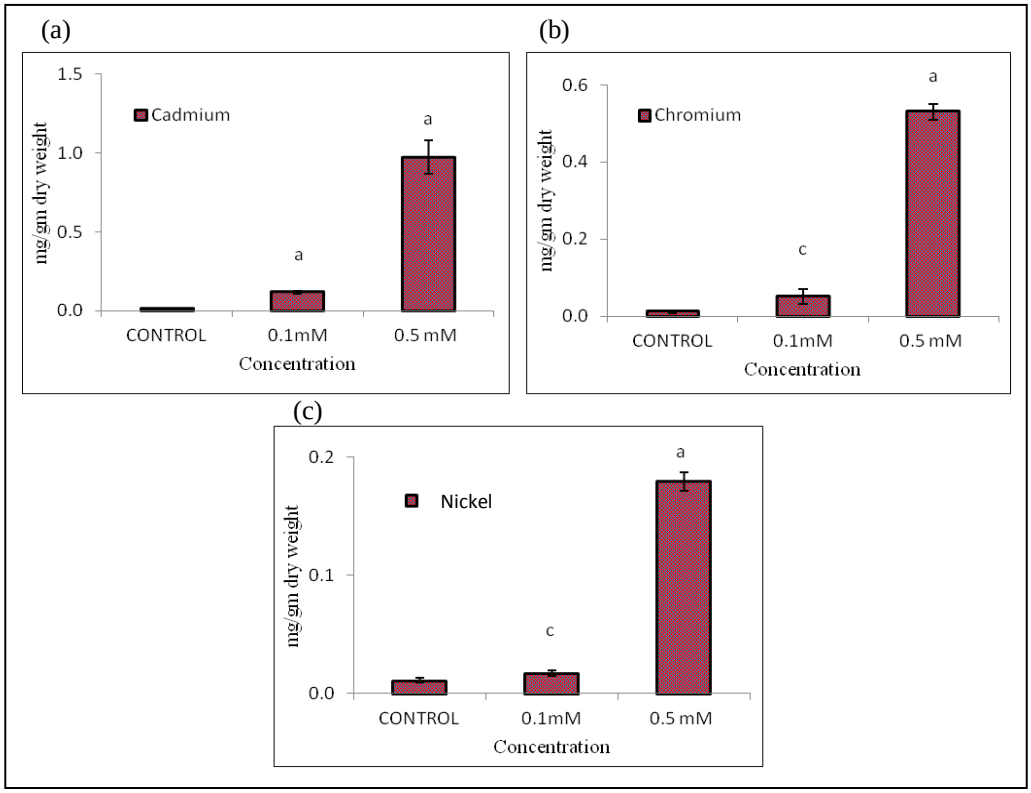

Figure 24: Atomic absorption spectroscopic analysis (AAS) of metals (Cd, Cr, Ni) in the dry biomass of metal resistant *Bacillus cereus* NI40215.

Values are expressed as Mean of three independent observations. $^{a}P \leq 0.001$ compared to control reaction; $^{b}P \leq 0.01$ compared to control reaction; $^{c}P \leq 0.05$ compared to control reaction.

Table 10: AAS data of metal ions in the dry biomass of metal resistant *Bacillus cereus* NI40215.

Conc.	Cd Mean ± S D	Cr Mean ± SD	Ni Mean ± SD
CONTROL	0.011 ± 0.003	0.011 ± 0.004	0.011 ± 0.002
0.1mM	0.115 ± 0.008 [a]	0.050 ± 0.019 [c]	0.017 ± 0.003 [c]
0.5 mM	0.974 ± 0.108 [a]	0.531 ± 0.021 [a]	0.179 ± 0.008 [a]

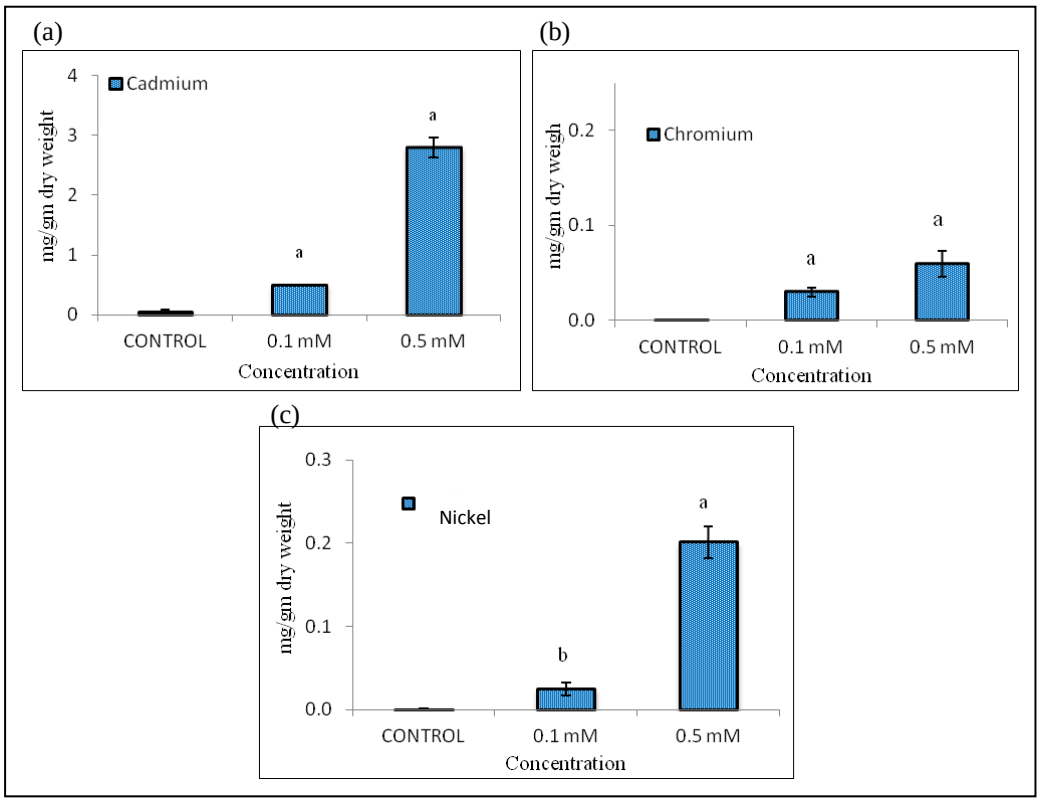

Figure 25: ICP-OES analysis of metal ions in the dry biomass of metal resistant *Pseudomonas aeruginosa* RV3.

Values are expressed as Mean of three independent observations. $^{a}P \leq 0.001$ compared to control reaction; $^{b}P \leq 0.01$ compared to control reaction; $^{c}P \leq 0.05$ compared to control reaction.

Table 11: ICP-OES data of metal ions in dry biomass of metal resistant *Pseudomonas aeruginosa* RV3

Conc.	Cd Mean ± SD	Cr Mean ± SD	Ni Mean ± SD
CONTROL	0.052 ± 0.037	0.0006 ± 0.0001	0.0007 ± 0.0004
0.1 mM	0.499 ± 0.003 [a]	0.029 ± 0.007 [a]	0.025 ± 0.008 [b]
0.5 mM	2.792 ± 0.167 [a]	0.059 ± 0.014 [b]	0.201 ± 0.019 [a]

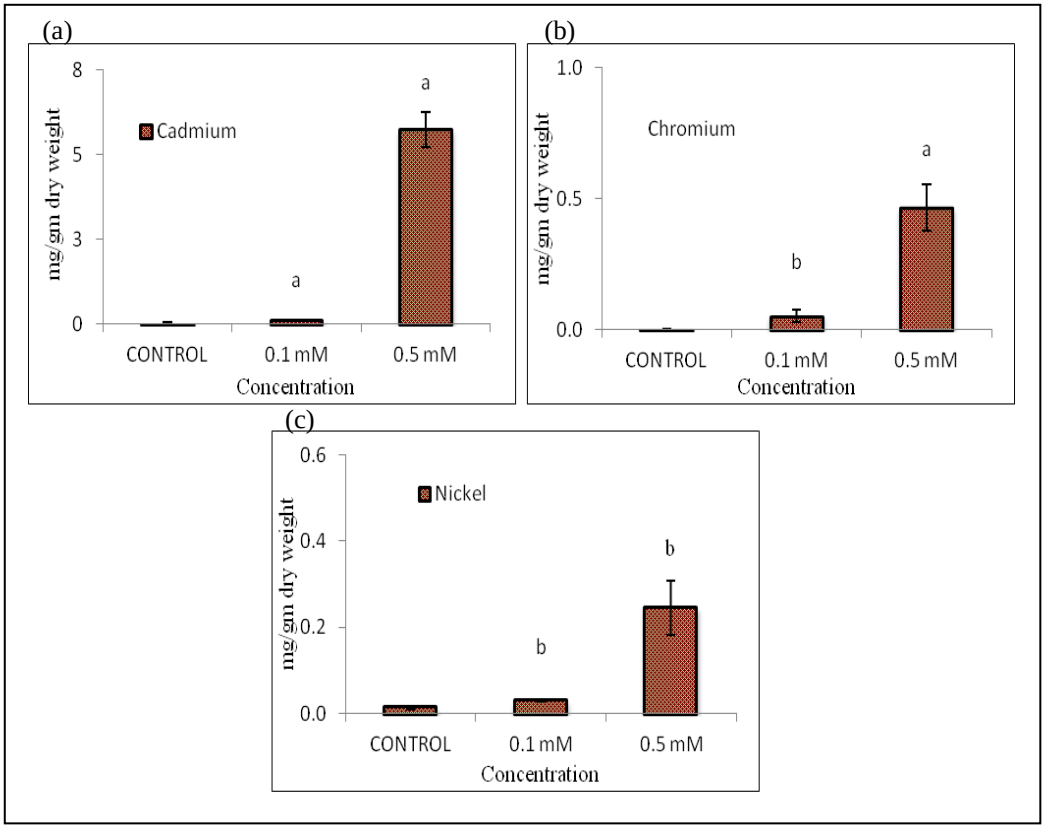

Figure 26: ICP-OES analysis of metal ions in the dry biomass of metal resistant *Bacillus cereus* NI40215.

Values are expressed as Mean of three independent observations. $^{a}P \leq 0.001$ compared to control reaction; $^{b}P \leq 0.01$ compared to control reaction; $^{c}P \leq 0.05$ compared to control reaction.

Table 12: ICP-OES data of metal ions in dry biomass of metal resistant *Bacillus cereus* NI40215

Conc.	Cd Mean ± SD	Cr Mean ± SD	Ni Mean ± SD
CONTROL	0.032 ± 0.013	0.0006 ± 0.0003	0.014 ± 0.004
0.1 mM	0.111 ± 0.009 [a]	0.053 ± 0.025 [c]	0.029 ± 0.003 [b]
0.5 mM	5.742 ± 0.517 [a]	0.467 ± 0.087 [a]	0.246 ± 0.063 [b]

4.7.1 Proteomic approach for identification of proteins expressed in response to heavy metals (Cd & Cr) using 2DGE and MALDI-TOF spectroscopy

Proteomics approach was used to identify the differentially expressed proteins in response to heavy metals (Cd & Cr). For this *Pseudomonas aeruginosa* RV3 strain was obtained from the chemostat and cultured in minimal medium in presence of metal as described in the methodology section. The proteins extracted from the bacterial cells were analyzed by 2D PAGE (IPG strips of pH range 3-10) and MALDI-TOF mass spectroscopy. The proteins expressed in response to Cd & Cr were as shown in (Figure 27 & 28).

In *Pseudomonas aeruginosa* RV3 treated with Cd (2mM), we have identified 11 protein spots that were either induced or differentially expressed as compared to untreated control (Figure 27). Based on the mascot scores, these proteins were identified as groEL (induced), prolyl-tRNA synthetase (induced), outer membrane porin F precursor (induced), ATP synthase subunit beta (induced), hypothetical protein PaerPA_01001816 (induced), binding protein of ABC transporter (differentially expressed), lipoyl synthase (induced), tRNA pseudouridine synthase A (induced), 50S ribosomal protein L3 (repressed), arginine repressor (differentially expressed) and putative heavy metal chaperone/transporter (induced) (Table 13). The identified proteins are involved in variety of cellular functions such as protein repair, translation, and maintenance of cell shape, ATP production, transportation and arginine synthesis and are found to be modulated in response to Cd treatment in the bacterium.

When *Pseudomonas aeruginosa* RV3 were treated with Cr (2 mM), we have identified 12 protein spots that were either induced or repressed or differentially expressed (Figure 28).

Based on the mascot score the proteins that are induced or differentially expressed were identified as chaperonin groEL (induced), atpD gene product (induced), L-isoaspartate O-methytransferase (induced), F0F1 ATP synthase (induced), 50S ribosomal protein L6 (induced), putative outer member protein (induced), czcC gene product (differentially expressed) and hypothetical protein HMPREF9505_02475 (induced). The proteins that were repressed in the Cr treated cells or present only in the untreated cells were identified as rpsA gene product, unnamed protein product, superoxide dismutase and transposase (Table 14). These proteins were also found to be involved in protein repair, ATP synthesis, ATP production, protein biosynthesis, cell envelope, Cd, Zn, Co resistance, antioxidant enzyme and translation in the bacterial cell and are modulated in response to Cr treatment.

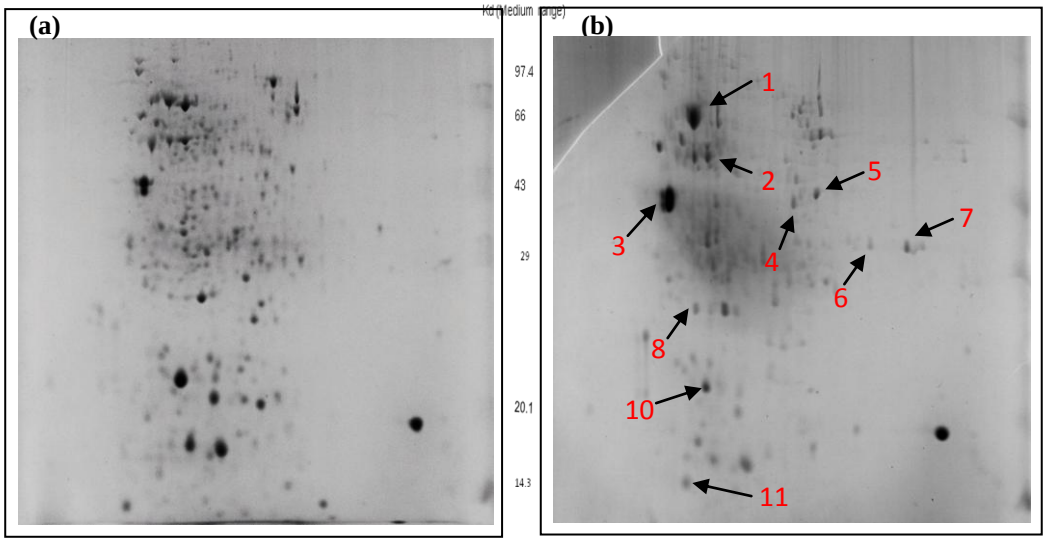

Figure 27: 2DGE analysis of protein expression pattern in the metal resistant *Pseudomonas aeruginosa* RV3 grown in (a) absence of Cd (control), (b) presence of Cd 2 mM.

Table 13: Identification of selected 2D protein spots from Cd (2 mM) treated ***Pseudomonas aeruginosa* RV3** by MALDI-TOF MS.

Spot No.	Accession No.	Protein	Score	Mass	Species	Function
1	gi|12230880	groEL protein	211	57107	*Pseudomonas aeruginosa*	Protein repair
2	gi|114152204	Prolyl-tRNA synthetase	32	64500	*Lactobaciluus salivarus*	Translation
3	gi|130680	Outer membrane porin F precursor	261	37844	*Pseudomonas aeruginosa*	Cell shape
4	gi|81857552	ATP synthase subunit beta	34	50417	*Neisseria meningitidis*	ATP production
5	gi|107100788	Hypothetical protein PaerPA_01001816	68	37358	*Pseudomonas aeruginosa*	Unknown
6	gi|15596539	Binding protein component of ABC transporter	62	33147	*Pseudomonas aeruginosa*	Transporter protein
7	gi|47117196	Lipoyl synthase	32	35803	*Nitrosomonas europaea*	Sulfur insertion
8	gi|13878837	tRNA pseudouridine synthase A	33	29127	*Lactococcus lactis*	Translation
9	gi|3915827	50S ribosomal protein L3	30	22212	*Borrelia burdorferi*	Translation
10	gi|61211526	Arginine repressor	30	17563	*Corynebacterium diphtheriae*	Regulates arginine biosynthesis genes
11	gi|163789973	Putative heavy metal-chaperone/transport protein	38	8120	*Carnobacterium* sp. AT7	Protein repair

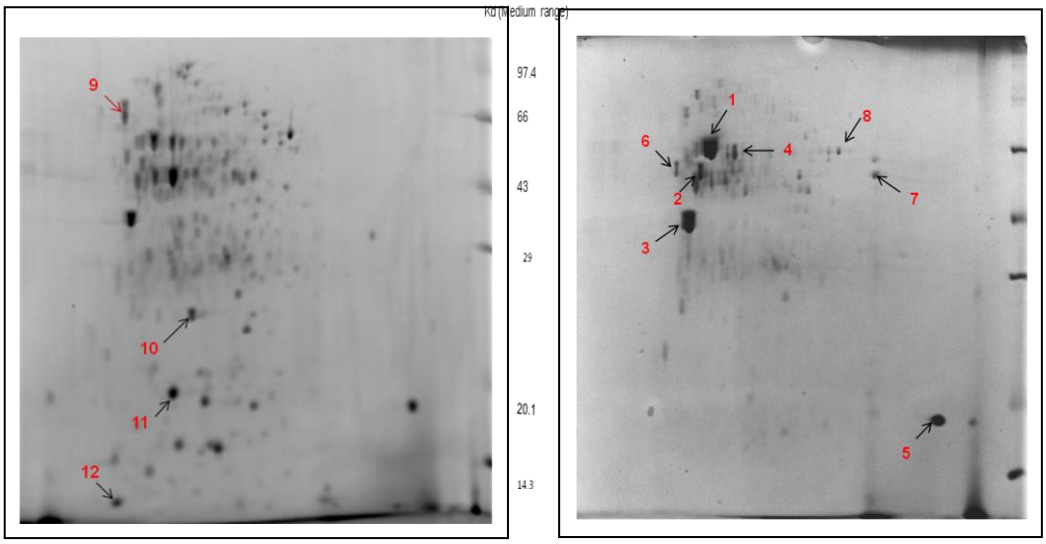

Figure 28: 2DGE analysis of protein expression pattern in the metal resistant *Pseudomonas aeruginosa* RV3 grown in (a) absence of Cr (control), (b) presence of Cr 2 mM

Table 14: Identification of selected 2D protein spots from control & Cr (2 mM) treated *Pseudomonas aeruginosa* RV3 by MALDI-TOF MS.

Spot No.	Accession No.	Protein	Mass	Score	Species	Function
1	gi|152986611	Chaperonin groEL	57019	172	*Pseudomonas aeruginosa* PAO1	Protein repair
2	gi|15600747	atpD gene product	49526	112	*Pseudomonas aeruginosa* PAO1	ATP synthesis
3	gi|289209616	L-isoaspartate O-methyltransferase	24471	73	*Thioalkalivibrio* sp.	Protein Repair
4	gi|375049654	F0F1 ATP synthase	55540	101	*Pcseudomonas aeruginosa* PAO1	ATP production
5	gi|221133731	50S ribosomal protein L6	18917	59	*Glaciecola* sp. HTCC2999	Protein biosynthesis
6	gi|313107399	Putative outer membrane protein	48772	126	*Pseudomonas aeruginosa* PAO1	Gram negative cell envelope
7	gi|15597718	czcC gene product	46880	46	*Pseudomonas aeruginosa* PAO1	Cd, Zn, Co resistance
8	gi|307289105	Hypothetical protein HMPREF9505_02475	5199	52	*Enterococcus* sp.	Unknown
9	gi|15598358	rpsA gene product	61946	118	*Pseudomonas aeruginosa* PAO1	Translation
10	gi|15598725	Unnamed protein product	21922	111	*Pseudomonas aeruginosa* PAO1	Unknown
11	gi|1529867 17	Superoxide dismutase	21466	71	*Pseudomonas aeruginosa* PA7	Attacks anion radicals
12	gi | 374096775	Transposase	4377	36	*Streptomyces hygroscopicus*	Movement of transposon

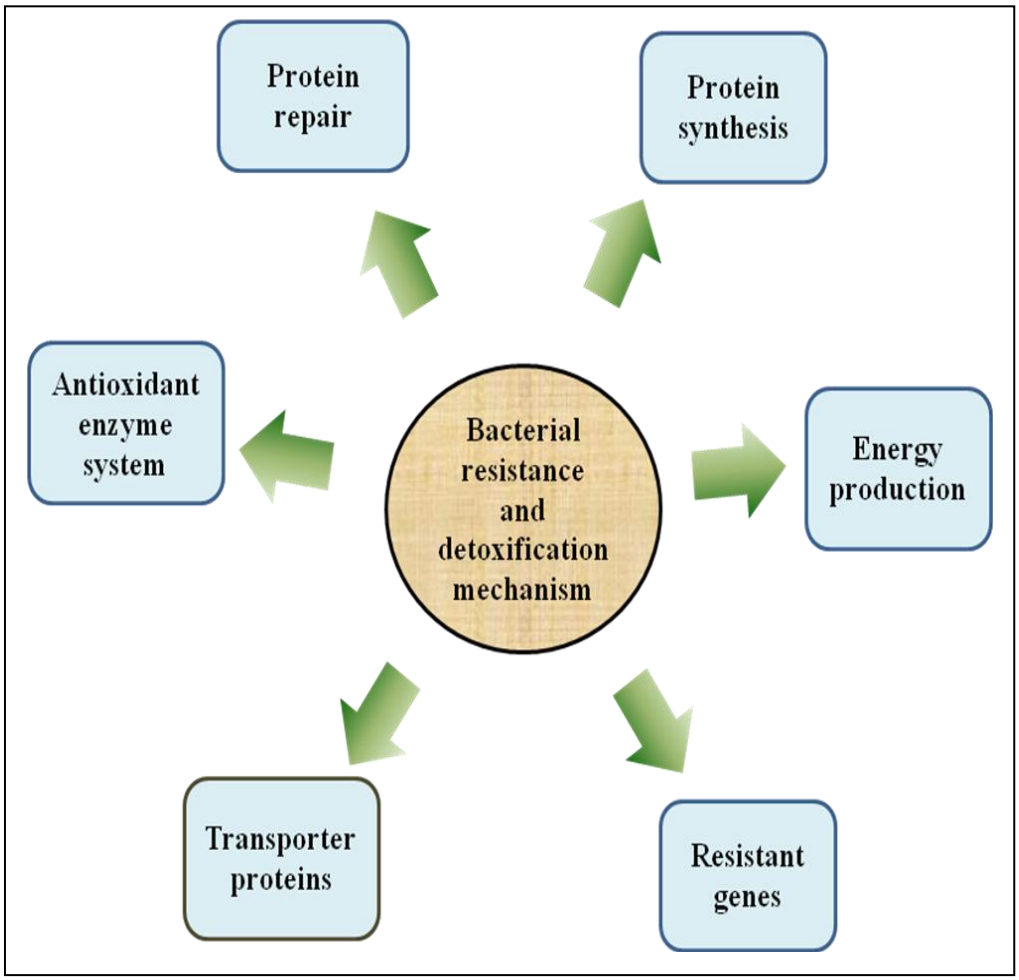

Figure 29: Mechanism of heavy metal detoxification in metal resistant bacterial strains.

4.8.1 Molecular cloning and characterization of gene encoding Lipoyl synthase identified by 2DGE method from *Pseudomonas aeruginosa* RV3.

Based on the proteomic studies, lipoyl synthase was found to be induced in response to Cd treatment, and very limited literature are available on the role of lipoyl synthase in the bacterial system, so the lipoyl synthase (*lipA*) gene from *Pseudomonas aeruginosa* RV3 was PCR amplified and cloned in InsTA cloning vector (Figure 30 & 31). The clones were confirmed with colony PCR and restriction digestion (Figure 32) and the cloned gene was sequenced and phylogenetic analysis revealed similarity with *lipA* gene of *Pseudomonas aeruginosa* (Figure 33).

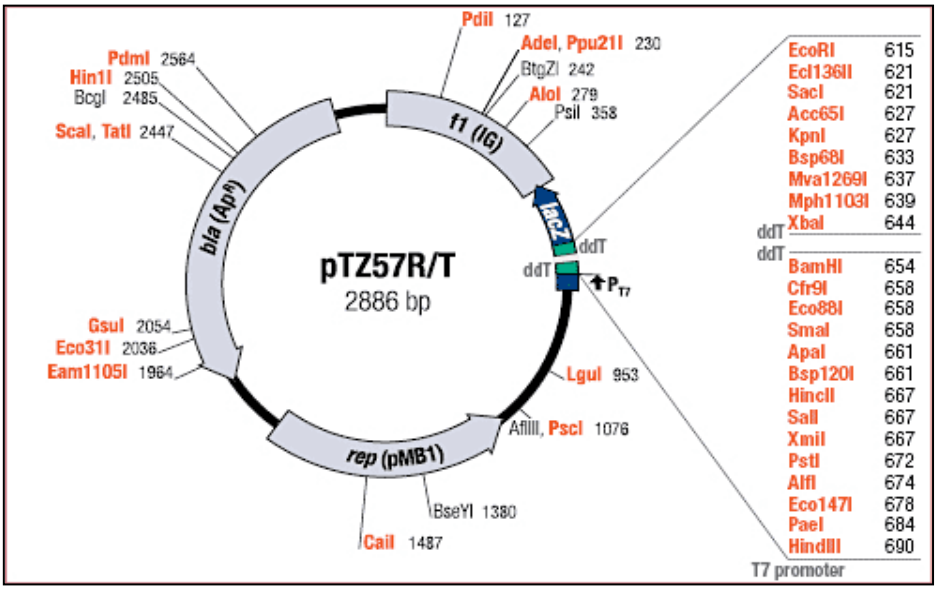

Figure 30: InsTA cloning vector restriction site map.

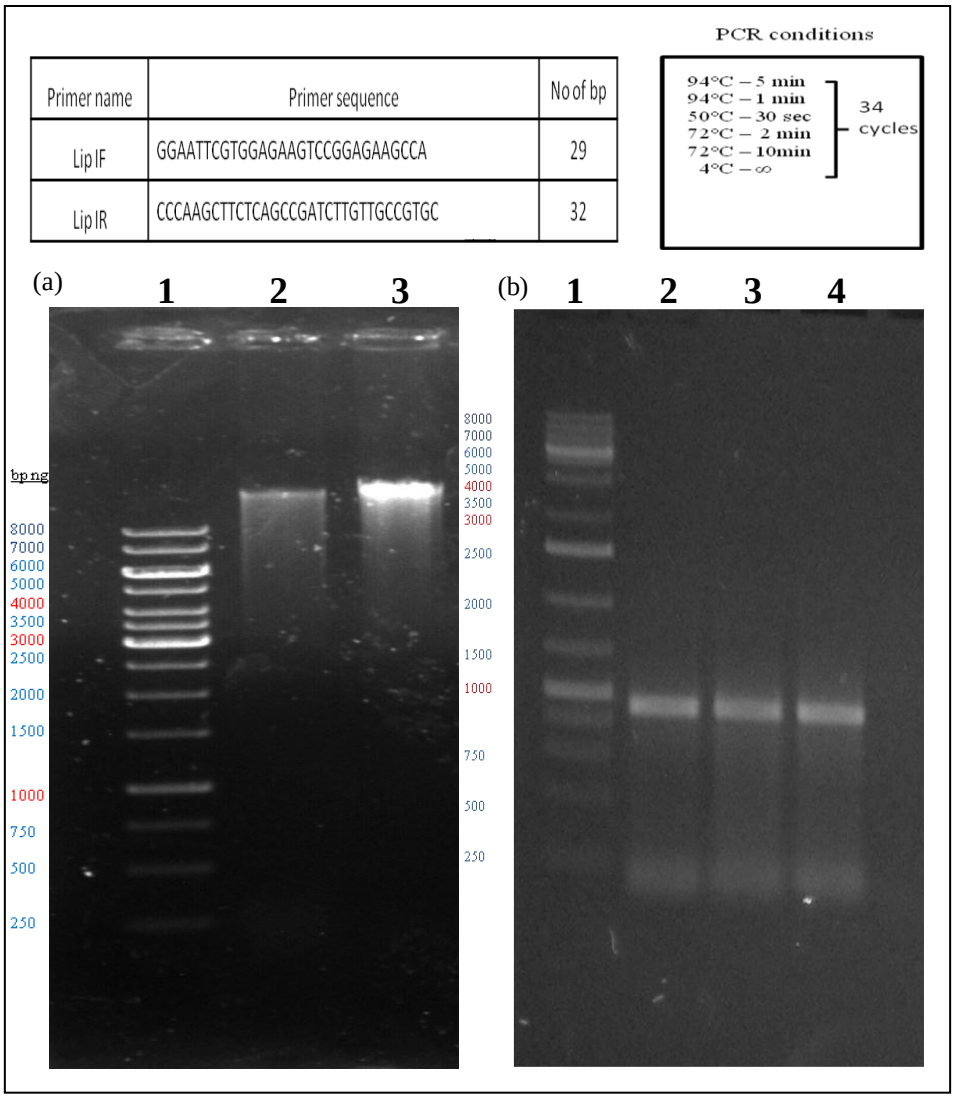

Primer name	Primer sequence	No of bp
Lip IF	GGAATTCGTGGAGAAGTCCGGAGAAGCCA	29
Lip IR	CCCAAGCTTCTCAGCCGATCTTGTTGCCGTGC	32

Figure 31: (a) Agarose gel analysis of genomic DNA of *Pseudomonas aeruginosa* RV3; Lane 1: 1kb ladder, Lane 2, 3: genomic DNA. (b) PCR amplified *lipA* gene of *Pseudomonas aeroginosa* RV3; Lane 1: 1kb ladder, Lane 2, 3 & 4: PCR amplification of 1 kb *lipA* gene.

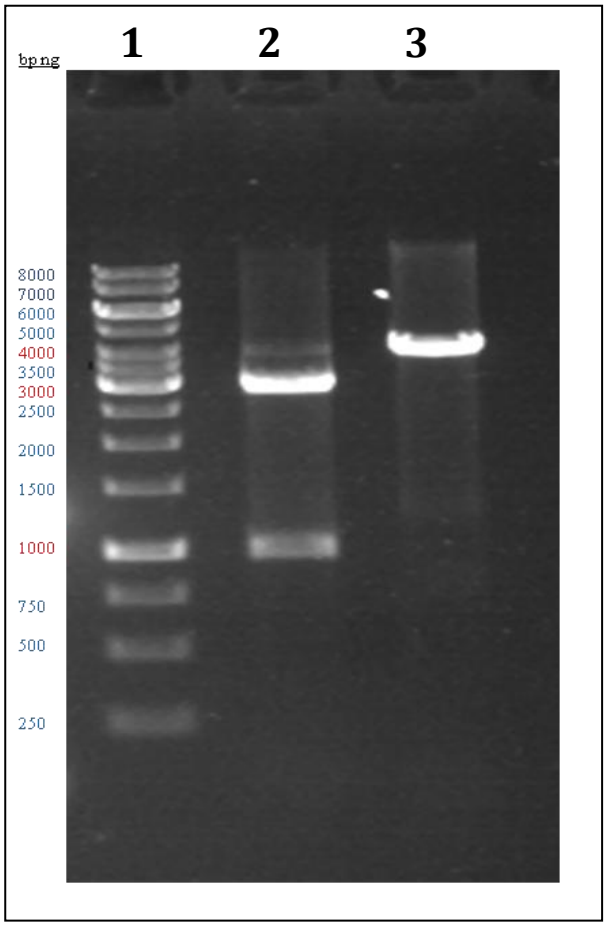

Figure 32: Agarose gel analysis of amplified *lipA* gene & InsTA vector by restriction digestion; Lane1: 1kb ladder, Lane 2: *lipA* cloned plasmid-+ EcoRI + HindIII (3kb vector, 1kb insert release), Lane 3: *lipA* cloned plasmid + EcoRI (4kb).

4.8.2 *In silico* prediction of LipA protein structure using bioinformatics tools.

The nucleotide sequence of the *lipA* gene is shown in Table15. The gene sequence was deposited in the NCBI GenBank database and assigned the accession No. KP334132. The BLAST result depicts the similarity and identity with *Pseudomonas aeruginosa* species (Table 17) and the phylogenetic tree was constructed using neighbor joining method (Figure 33). The translated amino acid sequence is shown in Table 16. Further a PDB BLAST search was performed against the translated *lipA* gene (Table 18) indicating that the amino acid sequence does not have a 3D structure and hence it was predicted using I-TASSER Server [218].

The I-TASSER server generated five 3D structure of the *lipA* gene (Figure 35). The predicted normalized B-Factor of the generated structures are shown in Figure 34. The Top ten templates used in predicted structure are shown in Table 19. Further the generated five modes were refined two times (Initial refinement and final refinement) using ModRefiner. The RMSD and TM-Score of the initial and final refinement compared to the initial model are shown in Table 20 [219, 220].

ANOLEA (Atomic Non-Local Environment Assessment) is a server that performs energy calculations on a protein chair evaluating the "Non- Local Environment" (NLE) of each heavy atom in the molecule. The web server can be accessed via the url link http://protein.bio.puc.cl/anolea/. The initial and final refined models of LipA were analyzed using the ANOLEA assessment server (Table21). Ramachandran plot analysis was carried out using RAMPAGE Server for the initial refined and final refined model (shown in Table 22) [221, 222]. The Ramachandran plot of the final refined model is shown in Figure 36.

Table 15: Detail parameters of the deposited sequence to NCBI GenBank

Description	**Parameters**
Accession	KP334132
Organism	*Pseudomonas aeruginosa* RV3
Author	Saikia, V. and Ramteke, A.
Title	Biochemical Characterization and Mechanistic Study of Heavy Metal Detoxification in the Metal Resistant Bacteria.
Base pair	972

>Lip A

GTGGAGAAGTCCGGAGAAGCCAAGCCGGGCAAGGTGGAAGTCGGCGTGAA
GCTGCGCGGCGCGGAAAAGGTCGCGCGGATTCCGGTGAAGATCATTCCCAC
CGAGGAACTGCCGAAGAAACCCGACTGGATCCGCGTGCGCATCCCGGTTTCC
CCCGAGGTCGACCGCATCAAGCAACTGCTGCGCAAGCACAAGCTGCACAGC
GTCTGCGAAGAGGCGTCCTGCCCGAACCTGGGCGAGTGCTTCTCCGGCGGCA
CCGCGACCTTCATGATCATGGGCGATATCTGCACCCGGCGCTGCCCGTTCTG
CGACGTCGGCCATGGCCGGCCGAAGCCGCTGGACGTCGACGAGCCGACCAA
CCTGGCCATCGCCATCGCCGACCTGCGGCTGAAGTACGTGGTGATCACCTCG
GTGGACCGCGACGACCTGCGCGACGGCGGCGCCCAGCACTTCGCCGACTGC
CTGCGCGAGATCCGCAAGCTGTCGCCGGGGATCCAGCTGGAAACCCTGGTGC
CCGACTATCGCGGTCGCATGGACATCGCCCTGGAGATCACCGCCAACGAGCC
GCCGGACGTGTTCAACCATAACCTGGAGACGGTGCCGCGCCTGTACCGCTCC
TCGCGGCCGGGCTCGGACTTCGAGTGGTCGCTGGACCTGCTGCAGAAGTTCA
AGCAGATGGTTCCGCACGTACCGACCAAGTCCGGGCTGATGCTCGGCCTGGG
CGAGACCGACGACGAGGTCATCGAGGTCATGCAGCGGATGCGCGAGCACGA
CATCGACATGCTGACCCTCGGCCAGTACCTGCAGCCGTCGCGCAACCACCTG
CCGGTGCAGCGCTTCGTGCATCCGGATACCTTCGCCTGGTTCGCCGAGGAAG
GCGAGAAGATGGGCTTCAAGAACGTCGCGTCCGGCCCGCTGGTGCGTTCGTC
CTACCATGCCGACCAGCAGGCGCACGGCAACAAGATCGGCTGA

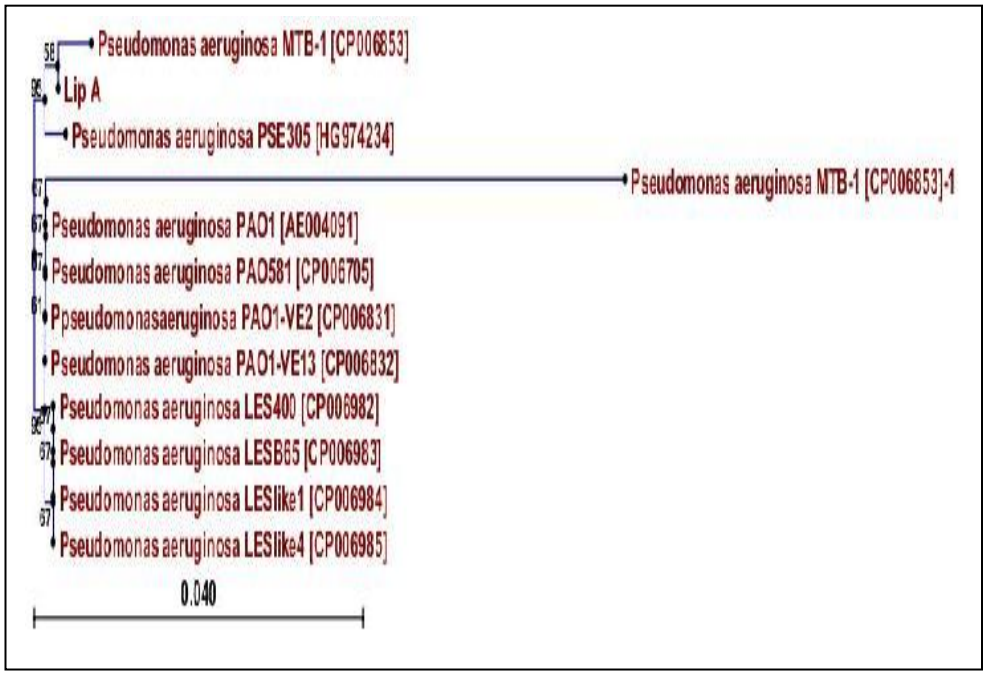

Figure 33: Phylogenetic tree was constructed using neighbor joining method and nucleotide distance measure of kimura 0.040 performing a bootstrap analysis of 100 replicates.

Table 16: Translated Sequence (Genetic Code-11: Bacterial and Plant Plastid, Frame Shift: +3)

>Lip A

VEKSGEAKPGKVEVGVKLRGAEKVARIPVKIIPTEELPKKPDWIRVRIPVS
PEVDRIKQLLRKHKLHSVCEEASCPNLGECFSGGTATFMIMGDICTRRCPF
CDVGHGRPKPLDVDEPTNLAIAIADLRLKYVVITSVDRDDLRDGGAQHF
ADCLREIRKLSPGIQLETLVPDYRGRMDIALEITANEPPDVFNHNLETVPR
LYRSSRPGSDFEWSLDLLQKFKQMVPHVPTKSGLMLGLGETDDEVIEVM
QRMREHDIDMLTLGQYLQPSRNHLPVQRFVHPDTFAWFAEEGEKMGFK
NVASGPLVRSSYHADQQAHGNKIG

Table 17: BLAST result showing similarity between the desired gene sequences with *Pseudomonas aeruginosa* species.

Sl No.	Accession	Description	Max Score	Total Score	Query cover	E-Value	Identity
1	CP006853.1	*Pseudomonas aeruginosa* MTB-1, complete genome	1777	1777	100%	0.0	99%
2	CP006832.1	*Pseudomonas aeruginosa* PAO1-VE13 genome	1777	1777	100%	0.0	99%
3	CP006831.1	*Pseudomonas aeruginosa* PAO1-VE2 genome	1777	1777	100%	0.0	99%
4	CP006705.1	*Pseudomonas aeruginosa* PAO581 genome	1777	1777	100%	0.0	99%
5	AE004091.2	*Pseudomonas aeruginosa* PAO1, complete genome	1777	1777	100%	0.0	99%
6	HG974234.1	*Pseudomonas aeruginosa* PSE305 genome	1777	1777	100%	0.0	99%
7	CP006985.1	*Pseudomonas aeruginosa* LESlike4 sequence	1777	1777	100%	0.0	99%
8	CP006984.1	*Pseudomonas aeruginosa* LESlike1 sequence	1777	1777	100%	0.0	99%
9	CP006983.1	*Pseudomonas aeruginosa* LESB65 sequence	1777	1777	100%	0.0	99%
10	CP006982.1	*Pseudomonas aeruginosa* LES400 sequence	1777	1777	100%	0.0	99%

Table 18: PDB BLAST result description detail run against LipA.

Sl No.	Accession	Description	Max Score	Total Score	Query cover	E-Value	Identity
1	4U0O_B	Chain B, Crystal Structure Of *Thermosynechococcus elongatus* Lipoyl Synthase 2 Complexed With Mta And Dtt [*Thermosynechococcus elongatus* BP-1]	263	263	85%	2e-85	47%
2	4JY8_A	Chain A, X-ray Snapshots Of Possible Intermediates In The Time Course Of Synthesis And Degradation Of Protein-bound Fe4s4 Clusters [*Thermotoga maritima* MSB8]	38.1	38.5	60%	0.006	25 %
3	3IIZ_A	Chain A, X-Ray Structure Of The Fefe-Hydrogenase Maturase Hyde From T. *maritima* In Complex With S-Adenosyl-L-Methionine [*Thermotoga maritima*]	38.1	38.1	60%	0.007	25 %
4	4JYD_A	Chain A, X-ray Snapshots Of Possible Intermediates In The Time Course Of Synthesis And Degradation Of Protein-bound Fe4s4 Clusters [*Thermotoga maritima* MSB8]	38.1	38.1	60%	0.007	25 %
5	3CIW_A	Chain A, X-Ray Structure Of The [fefe]-Hydrogenase Maturase Hyde From *Thermotoga maritima* [*Thermoto gamaritima*]	38.1	38.1	60%	0.007	25 %
6	4JY9_A	Chain A, X-ray Snapshots Of Possible Intermediates In The Time Course Of Synthesis And Degradation Of Protein-bound Fe4s4 Clusters [*Thermotoga maritima* MSB8]	38.1	38.1	60%	0.007	24%
7	3CIX_A	Chain A, X-ray Structure Of The [fefe]-hydrogenase Maturase Hyde From *Thermotoga maritima* In Complex With Thiocyanate [*Thermotoga maritima*]	38.1	38.1	60%	0.007	24%
8	1R30_A	Chain A, The Crystal Structure Of Biotin Synthase, An S- Adenosyl methionine-dependent Radical Enzyme [*Escherichia coli*]	37.4	37.4	17%	0.012	36%
9	2KEY_A	Chain A, Solution Nmr Structure Of A Domain From A Putative Phage Integrase Protein Bf2284 From *Bacteroides fragilis*, Northeast Structural Genomics Consortium Target Bfr257c [*Bacteroides fragilis* NCTC 9343]	28.9	28.9	20%	2.6	25%
10	4E5Y_A	Chain A, Structure Of Human Fx Protein, The Key Enzyme In The Biosynthesis Of Gdp-l-fucose [*Homo sapiens*]	29.6	29.6	28%	3.2	26%

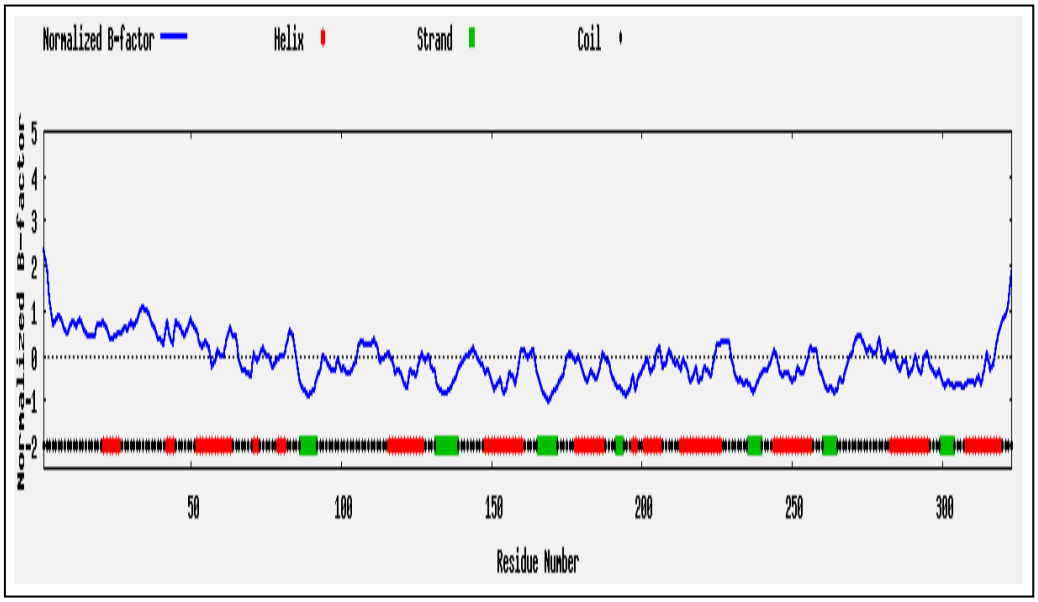

Figure 34: Predicted normalized B-Factor of the five generated models.

Table 19: Top 10 template hits used by the I-TASSER server

Sl No.	Rank[a]	PDB Hit	Norm Z score[b]
1	1	4u0oB	2.79
2	2	4u0pA	4.76
3	3	4u0oB	4.41
4	4	4u0oB	4.34
5	5	4u0oB	4.91
6	6	4u0oB	3.71
7	7	4u0oB	5.93
8	8	4u0oB	5,86
9	9	4u0oB	3.74
10	10	4u0oB	3.06

a- Rank of templates represents the top ten threading templates used by I-TASSER.

b- Norm. Z-score is the normalized Z-score of the threading alignments. Alignment with a Normalized Z-score >1 mean a good alignment and vice-versa.

Table 20: RMSD and TM Score of the initial and final refined models.

Sl No.	Name	Initial Refinement		Final Refinement	
		RMSD	**TM- Score to initial model**	**RMSD**	**TM- Score to initial refinement**
1	Model-1	0.917	0.9825	0.272	0.9983
2	Model-2	1.167	0.9765	0.262	0.9984
3	Model-3	0.718	0.9891	0.279	0.9982
4	Model-4	0.622	0.9914	0.323	0.9976
5	Model-5	0.955	0.9811	0.447	0.9957

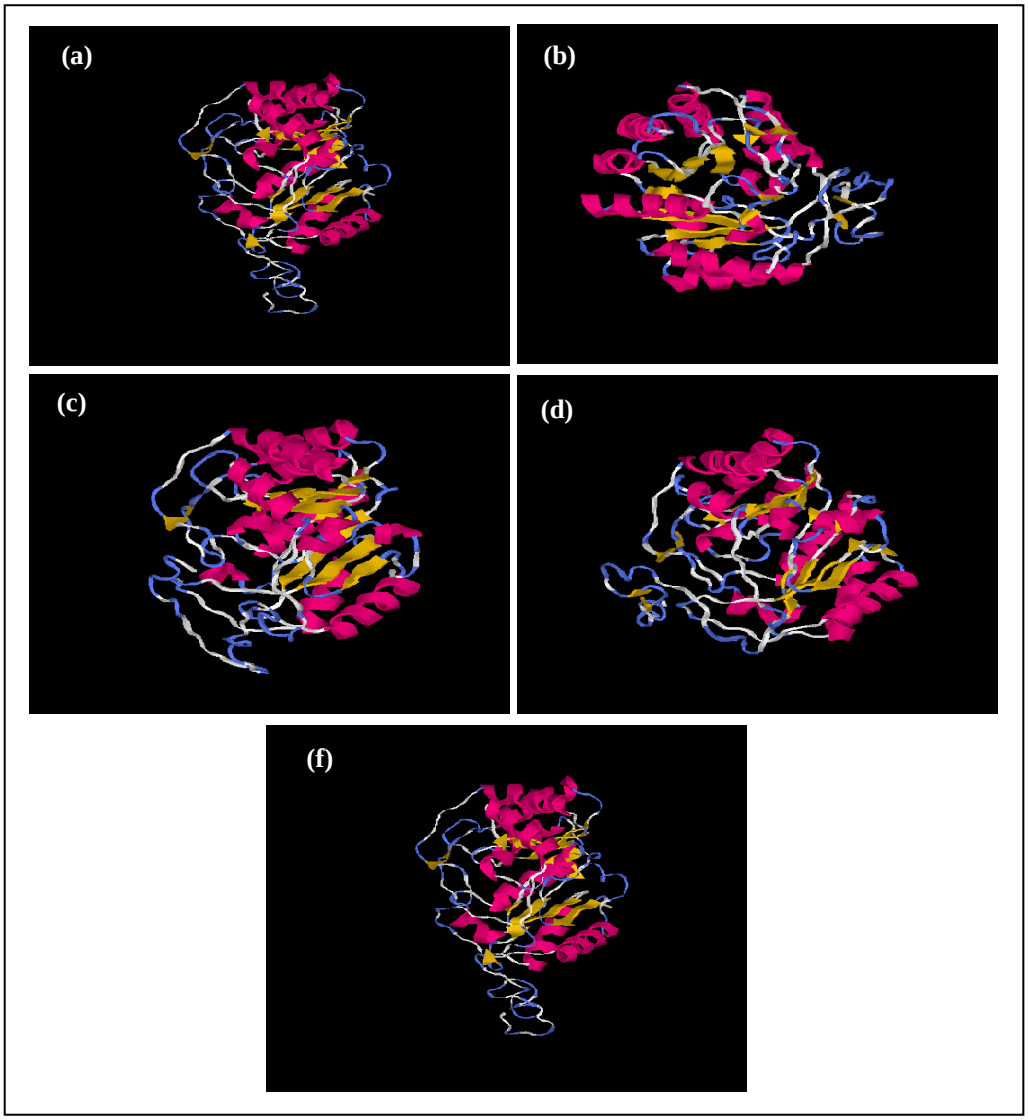

Figure 35: 3D visualization of Secondary structure of the final refined LipA.

Table 21: ANOLEA assessment analysis of initial refinement and final refinement

Sl. No.	Name	Energy[a] (E/KT units)		ANOLEA Z score[b]		No. of high energy amino acids		% High amino acids	
		Initial	Final	Initial	Final	Initial	Final	Initial	Final
1	Model-1	-1324	-854	2.65	3.47	49	90	15.17	27.86
2	Model- 2	-2181	-1551	0.84	1.99	30	44	9.29	13.62
3	Model-3	-2298	-1601	0.66	1.97	36	55	11.15	17.03
4	Model- 4	-2252	-1204	0.77	2.67	29	67	8.98	20.74
5	Model- 5	-2095	-1250	0.87	2.50	41	81	12.69	25.08

a- Total non-local energy of the protein (E/kT units)

b- Non-local normalized energy Z-score

Table 22: Ramachandran plot analysis of the initial and final refined model.

Sl. No.	Name	Residues in favoured region		Residues in allowed region		Residues in outlier region		Max deviation		Bad contacts	
		Initial	Final	Initial	Final	Initial	Final	Initial	Final	Initial	Final
1	Model- 1	261 (81.3%)	299 (93.%)	32 (10.%)	13 (4.0%)	28 (8.7%)	9 (2.8%)	23.2	14.2	5	33
2	Model- 2	258 (80.4%)	290 (90.%)	39 (12.%)	23 (7.2%)	24 (7.5%)	8 (2.5%)	15.0	16.7	0	19
3	Model- 3	254 (79.%)	292 (91.%)	32 (10%)	22 (6.9%)	35 (10%)	7 (2.2%)	19.1	14.0	6	18
4	Model- 4	262 (81.6%)	299 (93.1%)	36 (11.2%)	17 (5.3%)	23 (7.2%)	5 (1.6%)	19.4	18.6	4	15
5	Model- 5	253 (78.8%)	290 (90.3%)	41 (12.8%)	24 (7.5%)	27 (8.4%)	7 (2.2%)	17.8	14.8	1	19

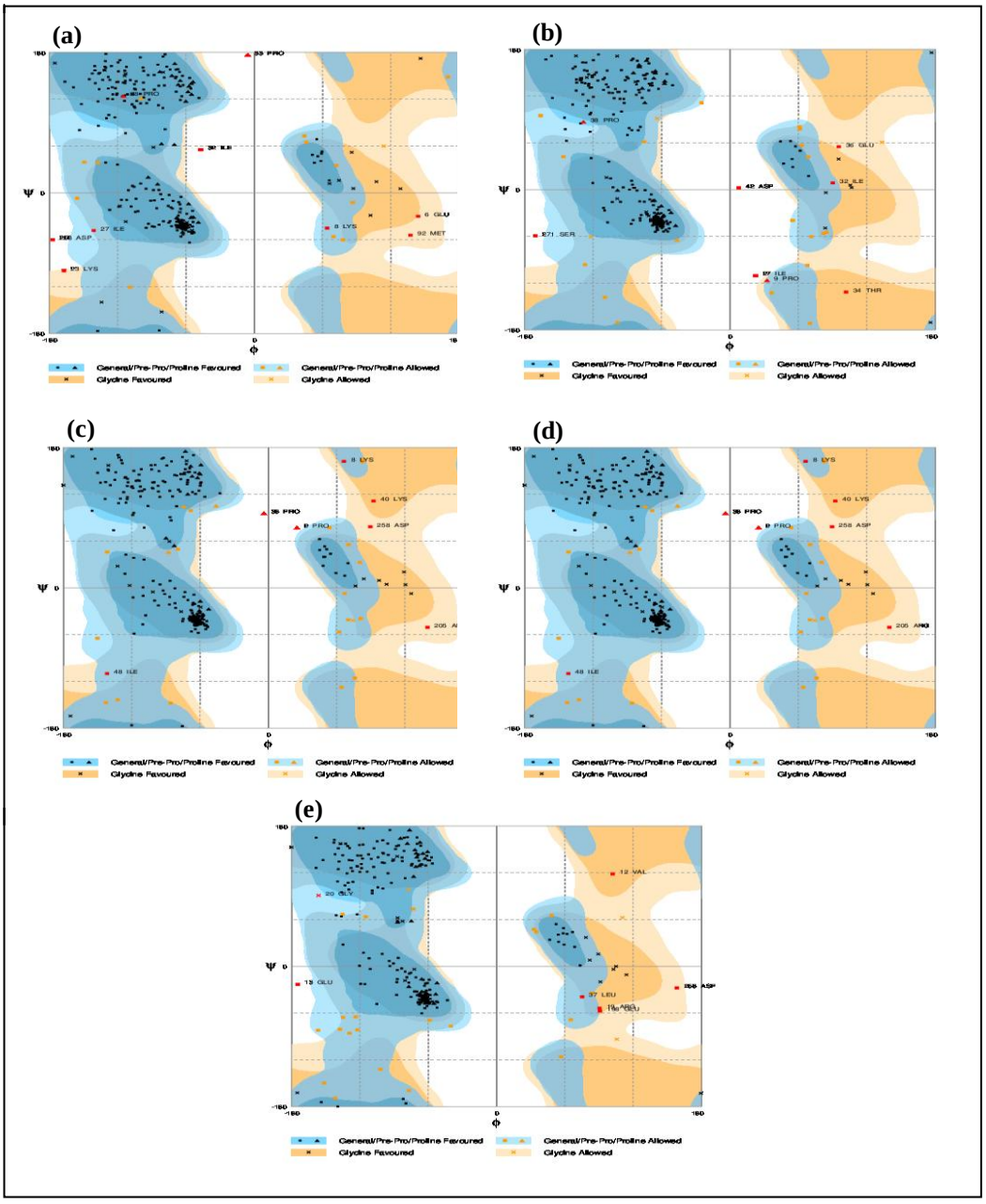

Figure 36: Ramachandran plot of the final refined model generated using RAMPAGE Server (a) Final 1 (b) Final 2 (c) Final 3 (d) Final 4 (e) Final 5.